A Central Role for Nicotinic Cholinergic Regulation of Growth Factor–Induced Endothelial Cell Migration

Martin K.C. Ng, Jenny Wu, Edwin Chang, Bing-yin Wang, Regina Katzenberg-Clark, Akiko Ishii-Watabe, John P. Cooke

Objective—An endothelial nicotinic acetylcholine receptor (nAChR) participates in atherogenesis and tumorigenesis by promoting neovascularization. To date, the mechanisms of nAChR-mediated angiogenesis and their relationship to angiogenic factors, eg, VEGF and bFGF, are unknown.

Methods and Results—Nicotine induced dose-dependent human microvascular endothelial cell (HMVEC) migration, a key angiogenesis event, to an extent which was equivalent in magnitude to bFGF (10 ng/mL) but less than for VEGF (10 ng/mL). Unexpectedly, nAChR antagonism not only abolished nicotine-induced HMVEC migration but also abolished migration induced by bFGF and attenuated migration induced by VEGF. Transcriptional profiling identified gene expression programs which were concordantly regulated by all 3 angiogens (nicotine, VEGF, and bFGF), a notable feature of which includes corepression of thioredoxin-interacting protein (TXNIP), endogenous inhibitor of the redox regulator thioredoxin. Furthermore, TXNIP repression by all 3 angiogens induced thioredoxin activity. Silencing thioredoxin by small interference RNA abrogated all angiogen-induced migration while silencing TXNIP strongly induced HMVEC migration. Interestingly, nAChR antagonism abrogates growth factor (VEGF and bFGF)–mediated induction of thioredoxin activity.

Conclusions—Nicotine promotes angiogenesis via stimulation of nAChR-dependent endothelial cell migration. Furthermore, growth factor–induced HMVEC migration, a key angiogenesis event, requires nAChR activation—an effect mediated in part by nAChR-dependent regulation of thioredoxin activity. (*Arterioscler Thromb Vasc Biol.* 2007;27: 106-112.)

Key Words: nicotine ■ angiogenesis ■ endothelium ■ vascular endothelial growth factor ■ fibroblast growth factor

The nicotinic acetylcholine receptor (nAChR) is a pentameric ligand-gated cationic channel.[1] The nAChR was first described in neurons, but has recently been identified in many cell types including endothelial cells (ECs) and vascular smooth muscle cells.[2] Intriguingly, ECs also synthesize and store acetylcholine.[3] Recently, we serendipitously discovered that nAChR activation causes ECs to form capillary tubes in vitro, and promotes angiogenesis in vivo.[4,5]

Pathological as well as physiological forms of angiogenesis are mediated by EC nAChRs. For example, by activating the EC nAChR, nicotine accelerates tumor angiogenesis and tumor growth in a murine Lewis lung cancer model.[4] The acceleration of tumor growth by environmental tobacco smoke is also mediated by nAChR-induced angiogenesis.[6] Furthermore, nAChR activation by nicotine stimulates the neovascularization and progression of atherosclerotic plaque.[4] On the other hand, activation of the nAChR in a murine model of diabetic ulceration enhances wound angiogenesis and healing.[7]

To date, the mechanisms of nAChR-mediated angiogenesis and their relationship to established angiogenic growth factors, such as VEGF and bFGF, are unknown. We therefore sought to study and compare the effects of nAChR activation on EC migration, a key event in angiogenesis, alongside those induced by VEGF or bFGF. In this article, we report an unexpected observation: pharmacological antagonism of the nAChR fully blocks bFGF-induced EC migration, and substantially suppresses the endothelial response to VEGF. Furthermore, by microarray analysis, we identify gene expression programs which are concordantly regulated by nicotine, VEGF, or bFGF, and confirm the role of one of these genes in the cholinergic component of growth factor-induced endothelial cell migration.

Methods

For Methods, please refer to the Data Supplement, available online at http://atvb.ahajournals.org.

Original received April 6, 2006; final version accepted October 16, 2006.

From the Department of Medicine (M.K.C.N., J.W., E.C., B.-y.W., R.K.-C., A.I.-W., J.P.C.), Division of Cardiovascular Medicine, Stanford University School of Medicine, Stanford, Calif.; and the Department of Cardiology (M.K.C.N.), Royal Prince Alfred Hospital, Sydney, NSW, Australia.

M.K.C.N. and J.W. contributed equally to this work

Correspondence to John P. Cooke, Falk Cardiovascular Research Center, Stanford University School of Medicine, 300 Pasteur Drive, Stanford, CA 94305-5406. E-mail john.cooke@stanford.edu

Arterioscler Thromb Vasc Biol. is available at http://www.atvbaha.org

DOI: 10.1161/01.ATV.0000251517.98396.4a

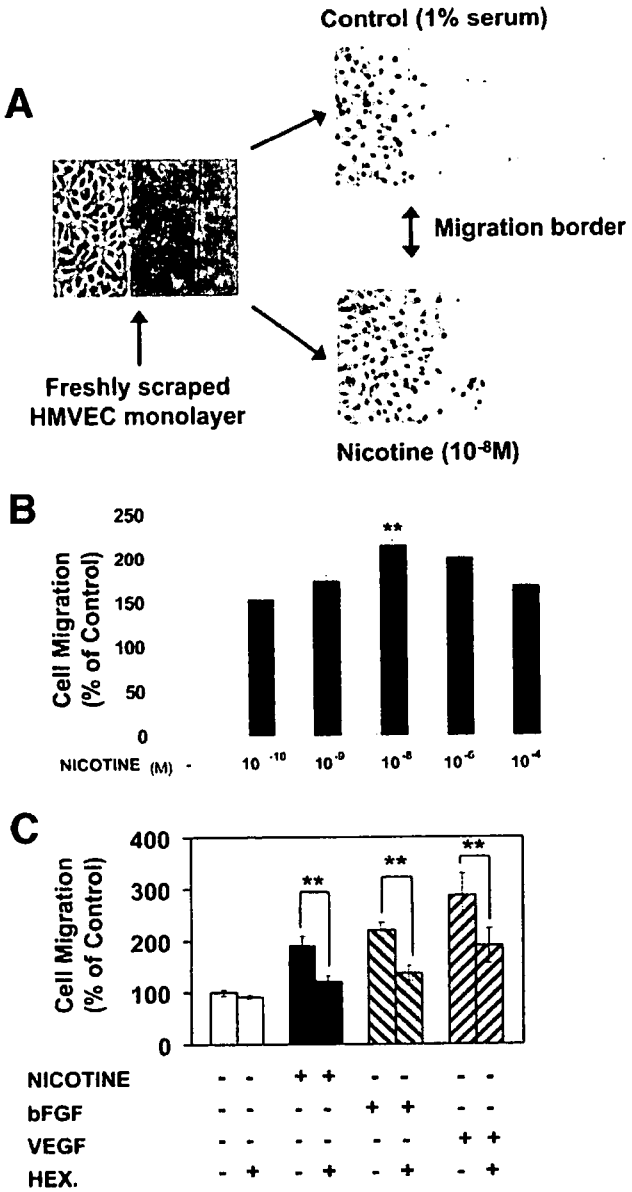

Figure 1. Role of nAChR in human microvascular endothelial cell (HMVEC) migration. A, Representative microphotographs of the HMVEC migration assay: after wounding of the monolayer with a razor blade, HMVECs migrate into the denuded area. B, Nicotine stimulates dose-dependent HMVEC migration which is maximal at a nicotine concentration of 10^{-8} mol/L ($P<0.001$ vs control). C, Effects of hexamethonium (HEX), a nAChR antagonist, on HMVEC migration induced by nicotine (10^{-8} mol/L), VEGF (10 ng/mL), and bFGF (10 ng/mL). Values are expressed as a percentage of migrating cells per high-powered field in vehicle-treated wells. $^{**}P<0.001$.

Results

A Cholinergic Component of Growth Factor–Mediated Endothelial Cell Migration

The effects of nicotine on human microvascular endothelial cell (HMVEC) migration were studied using standard wounding migration assays. Figure 1A depicts typical microphotographs of in vitro HMVEC migration in the presence of vehicle or nicotine. Nicotine stimulated EC migration in a dose-dependent manner with maximal stimulation at 10^{-8} mol/L, producing cell migration that was 216±9% that of vehicle-treated ECs ($P<0.001$ versus control; Figure 1B). Stimulation with VEGF or bFGF also induced EC migration with maximal effects at 10 ng/mL (data not shown). Nicotine-induced EC migration at 10^{-8} mol/L was equivalent in magnitude to that observed for bFGF (10 ng/mL) but less than for VEGF (10 ng/mL; P=NS for nicotine versus bFGF; $P<0.01$ for nicotine versus VEGF; Figure 1C). To further investigate the effects of nAChR-dependent pathways on EC migration, we studied the effect of the nAChR antagonist, hexamethonium (HEX, 10^{-4} mol/L), on EC migration induced by nicotine, VEGF, and bFGF. Hexamethonium abrogated nicotine-induced EC migration (Figure 1C). Unexpectedly, in addition to abolishing NIC-induced EC migration, HEX abolished migration induced by bFGF (P=NS versus control) and reduced migration induced by VEGF ($P<0.01$ for VEGF+HEX versus VEGF alone; Figure 1C). Similar results were observed with the nAChR antagonist, mecamylamine (10^{-6} mol/L; supplemental Figure I). The nAChR-related effect was dose-dependent: in the case of VEGF, cell migration was attenuated by 26±12%, 43±9%, and 52±12% by HEX concentrations of 10^{-8} mol/L, 10^{-6} mol/L, and 10^{-4} mol/L, respectively ($P<0.05$ for trend). Nicotinic receptor activation is known to stimulate EC proliferation.[4] Interestingly, nAChR antagonism also significantly attenuated VEGF- and bFGF-mediated EC proliferation as assessed by bromodeoxyuridine incorporation (supplemental Figure II). The nAChR antagonist-related effects were not the result of cellular toxicity as addition of hexamethonium or mecamylamine alone did not induce cell death as examined via 3-[4,5-dimethylthiazol-2-yl]-2,5-diphenyl tetrazolium bromide (MTT) assays, nor did mecamylamine or hexamethonium induce apoptosis in VEGF- or bFGF-treated cells as assessed by annexin V staining (data not shown).

Previous in vitro and in vivo data have implicated a central role for the α7-nAChR isoform in mediating nAChR-induced neovascularization.[5] Consistent with this, selective inhibition of the α7-nAChR isoform by α-bungarotoxin (10^{-9} mol/L) abrogated nicotine effects (P=NS versus control) and significantly attenuated bFGF and VEGF-induced EC migration by 50±11% and 38±13%, respectively ($P<0.05$ for stimulus versus stimulus + α-bungarotoxin; Figure 2A). We also studied HMVEC α7-nAChR mRNA expression in response to nicotine, VEGF, and bFGF over a 24-hour time course. At 1 hour, nicotine, VEGF, and bFGF all induced >10-fold downregulation of α7-nAChR expression compared with vehicle-treated conditions ($P<0.05$ versus control for all angiogens; Figure 2B). However, by 6 hours, there was significant upregulation of α7-nAChR expression by nicotine (12±0.8-fold), VEGF (11±1.3-fold), and bFGF (4±0.2-fold; $P<0.001$ versus control; Figure 2B). By 24 hours, HMVEC α7-nAChR expression in all conditions had returned to levels similar to control (P=NS versus control). These data suggest that nicotine, VEGF, and bFGF induce acute stimulation of α7-nAChR with subsequent early downregulation of α7-nAChR expression by negative feedback followed by upregulation at 6 hours. These findings are consistent with a role for nAChR in growth factor signaling pathways.

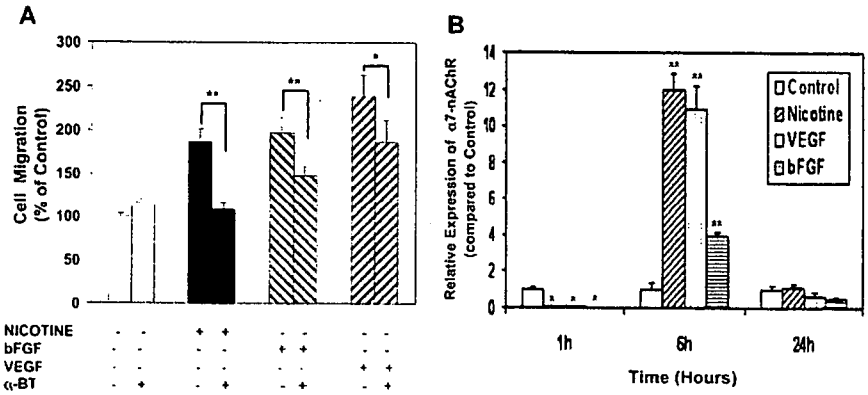

Figure 2. Role of the ∝7-nAChR isoform in growth factor–mediated EC migration. A, Effects of ∝-bungarotoxin (∝-BT), a specific inhibitor of the ∝7-nAChR isoform, on EC migration. Coadministration of ∝-BT (10^{-9} mol/L) abrogated the migragenic effects of nicotine (10^{-8} mol/L; P=NS vs control) and significantly attenuated the effects of bFGF (10 ng/mL) and VEGF (10 ng/mL). B, Effects of nicotine, VEGF, and bFGF on EC ∝7-nAChR expression at 1, 6, and 24 hours as assessed by relative real-time RT-PCR. *P<0.05; **P<0.001 compared with control.

Identification of Shared Transcriptional Responses to Nicotine, bFGF, and VEGF by Microarray Analysis

To further evaluate a cholinergic contribution to growth factor–induced EC migration, and to identify commonly regulated genes that may be required for HMVEC migration, we performed microarray analysis of HMVECs after exposure to nicotine, VEGF, or bFGF. At 24 hours after treatment, each of these stimuli induced profound transcriptional changes in HMVECs (Figure 3), resulting in differential expression of a total of 3072 genes uniquely identified by UniGene, as well as 312 expressed-sequence tags, all of which were represented by 4070 nonredundant cDNA clones. To study relationships between gene expression programs

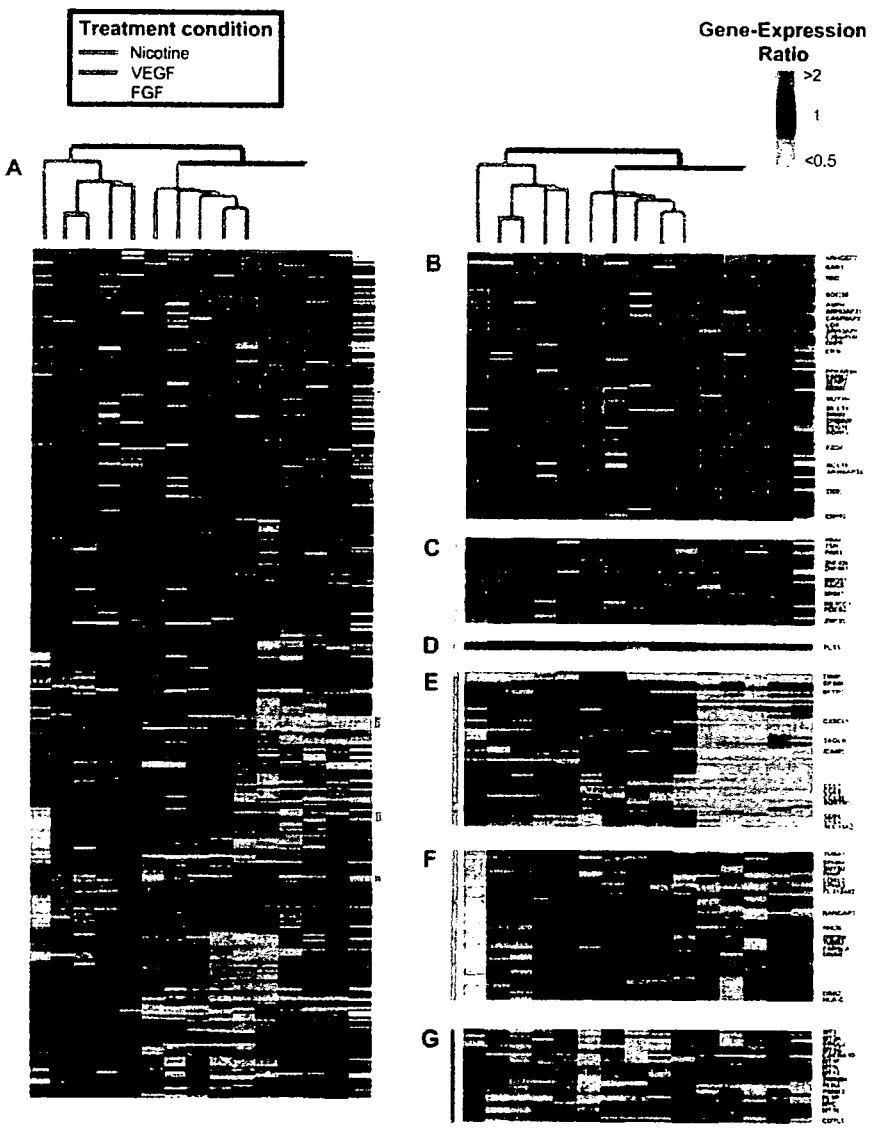

Figure 3. Hierarchical cluster analysis of transcriptional effects of nicotine, VEGF, or bFGF in human microvascular endothelial cells at 24 hours. A, Overview of the two way (genes against conditions) hierarchical cluster of 15 experiments (each condition was studied in quintuplicate) and 4070 nonredundant cDNA clones with significant change in expression at 24 hours. Data from individual elements or genes are represented in rows and experiments in columns. Red and green denote expression levels greater or less, respectively, than control values. Gray denotes technically inadequate or missing data. The intensity of the color reflects the magnitude of the change from baseline. The dendrogram above the matrix represents similarities in patterns of expression between experimental samples. B through G, Zoom boxes of concordantly expressed gene clusters, whose location are indicated by vertical colored bars adjacent to the dendrogram. Owing to space limitations, only genes discussed in the text are indicated by UniGene symbol.

induced by nicotine, VEGF, or bFGF, data for all differentially expressed genes at 24 hours were hierarchically clustered by gene and by array, thereby organizing genes and experimental samples on the basis of similarity of expression patterns (Figure 3A through 3F).[8] The cluster dendrogram shows that all 3 stimuli induced distinct transcriptional signatures which cluster within 3 distinct groups, but there is a closer relationship between the VEGF- and bFGF-induced expression profiles, which cluster together on the same dendrogram branch (Figure 3A).

Within the distinct transcriptional profiles induced by nicotine, VEGF, or bFGF, we identified 6 clusters with concordant gene expression (3 clusters of commonly activated and 3 commonly corepressed genes; Figure 3B through 3F). The characteristics of these clusters provide insights into shared cellular processes that may be requisite for angiogen-induced cell migration. The first activation cluster (Figure 3B), the "migration cluster," was enriched for genes associated with cytokinetic processes including migration-associated G protein signaling (Rho GTPase regulatory proteins and RIN2), integrin binding (ERBB2IP and ADAM9), cell cycle regulation and proliferation (RRM2, MDM2, AHR, MLLT4, and MUTYH), NF-κB activation (BCL10 and CASP8AP2), and migration-associated oxidoreductase activity (LOX and ASPH). Significantly, three Rho GTPase activating proteins (GAPs) including ARHGAP5, ARHGAP21, and ARHGAP24 and one Rho guanine nucleotide exchange factor (GEF), ARHGEF7, were concordantly upregulated in this cluster. Rho GEFs and GAPs, by respectively controlling the activation and inactivation of small Rho GTPases (Cdc42 and Rac), regulate the orchestration of cytoskeletal and adhesive changes during cytokinesis.[9]

A smaller second coactivation cluster (Figure 3C) includes the p21-activated kinase PAK1, an effector for the Rho GTPases Rac and Cdc42, that facilitates cell migration by coordinating formation of new adhesions at the leading edge of the cell with detachment at the trailing edge.[10] Other genes in this activation cluster comprise zinc finger proteins and genes involved in nucleic acid metabolism. Interestingly, all three angiogens induced activation of the VEGF receptor, FLT1, an effect that was stronger for bFGF-treated cells than for nicotine or VEGF (Figure 3D, which contains 3 nonredundant cDNA clones for FLT1). In addition to the coinduction of FLT1 by all three stimuli, we found that several isoforms of nAChR subunits are upregulated by VEGF at 24 hours (supplemental Table 1), suggesting other potential synergistic interactions between VEGF and cholinergic signaling pathways.

The first repression cluster (Figure 3E) contains genes that are strongly downregulated by bFGF, many of which are also concordantly repressed by nicotine and VEGF. A dominant theme among concordantly repressed genes is the downregulation of chemokine genes (principally of CC class) involved leukocyte chemotaxis (CCL2, CCL7, CCL8, CCL20, and CX3CL). Another prominent feature is the robust repression of thioredoxin interacting protein (TXNIP) (Figure 3E), a protein that binds and inhibits thioredoxin, a major intracellular antioxidant. Other corepressed genes in this cluster have been implicated in apoptosis (TNFRSF1B, EP300), signal transduction (CD53, SQSTM1), and cell adhesion (ICAM1). The second repression cluster (Figure 3F) included two Ephrin receptors: EPHB4, a marker of venous differentiation and EPHA2, an inhibitor of cell migration which suppresses integrin function. Other genes within this group were associated with tumor suppression, microtubular polymerization, and signal transduction. The striking feature of the third cluster of corepressed genes is a strong enrichment for metallothioneins (MT1E, MT1F, MT1G, MT1L, MT1X, MT2A, and MT3; Figure 3G). Metallothioneins (MTs) comprise a superfamily of small cysteine-rich proteins with high affinity for metal ions and antioxidant activity. By serving as a cellular reservoir for zinc and copper, MTs regulate the function of proteins requiring these metals such as DNA and RNA polymerases, zinc finger transcription factors, and p53.[11] Other genes in this cluster are involved in diverse functions including cell proliferation/apoptosis (MYC, ERCC2), lipid transport (PTLP), calcium ion transport (CACNA1D), and actin binding (COTL1).

In summary, the transcriptional signatures of nicotine, VEGF, and FGF, while distinct, demonstrate many overlapping features. By hierarchical cluster analysis, we have identified a series of shared angiogen-dependent EC transcriptional programs, with implications for understanding shared mechanisms in EC migration/angiogenesis.

Role of Thioredoxin Interacting Protein in the Cholinergic Contribution to Growth Factor–Induced EC Migration

As nAChR antagonism modulates VEGF- and bFGF-dependent EC migration, we hypothesized that some of the transcriptional effects shared by nicotine, VEGF, and bFGF may be nAChR-dependent. Thioredoxin interacting protein (TXNIP), a gene not previously associated with EC migration, was downregulated by all three angiogens. TXNIP is the endogenous inhibitor of thioredoxin. Thioredoxin is a major redox regulator of protein function increasingly implicated in tumorigenesis.[12,13] In microarray data from 3 nonredundant cDNA clones for TXNIP, nicotine, VEGF, and bFGF consistently decreased TXNIP expression—a finding confirmed by RT-PCR, which demonstrated decreased expression by 42±4%, 33±6%, and 26±7% relative to control, respectively ($P<0.001$ for all stimuli; Figure 4A). As in vivo reduction of TXNIP expression in the order of 30% to 40% has been associated with >3-fold increases in thioredoxin activity,[14] we hypothesized that TXNIP downregulation may influence thioredoxin activity and play a role in angiogen-mediated EC migration.

Using a standard assay for thioredoxin activity,[15] we found that addition of nicotine or VEGF induced thioredoxin activity significantly above vehicle-treated cells ($P<0.001$ versus control for all stimuli; Figure 4B). The addition of bFGF induced a less robust ($P<0.05$ versus control) but significant increase in thioredoxin activity (Figure 4B). Notably, coadministration of hexamethonium inhibited nicotine-, VEGF-, or bFGF-induced thioredoxin activity (Figure 4B; $P<0.001$ for each stimulus versus stimulus + hexamethomium). Hexamethonium alone had no significant effect on thioredoxin activity. Consistent with these results, nAChR antagonism abrogated nicotine, VEGF, and bFGF-mediated repression of TXNIP mRNA expression (P=NS versus control for each stimulus + hexamethonium; Figure 4A). Transfection of small interference RNA (siRNA)

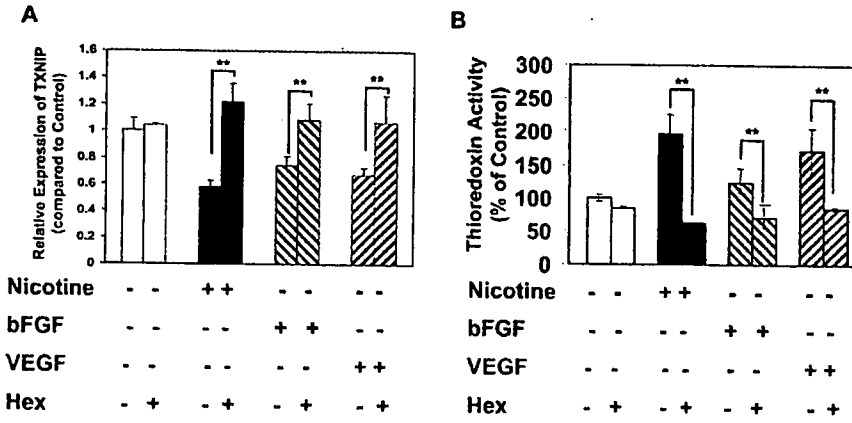

Figure 4. Role of nAChR in growth factor–mediated regulation of TXNIP expression and thioredoxin activity in ECs. Effects of nicotine (10^{-8} mol/L), VEGF (10 ng/mL), and bFGF (10 ng/mL) with/without coadministration of hexamethonium (10^{-4} mol/L) on TXNIP expression (A) and on thioredoxin activity (B) in human microvascular endothelial cells. Values for thioredoxin activity are expressed as a percentage of control (vehicle-treated cells). $^{**}P<0.01$.

against thioredoxin abrogated nicotine-, VEGF-, or bFGF-induced thioredoxin activity and abolished cell migration induced by nicotine, VEGF, or bFGF (P=NS versus control for each stimulus + siRNA; Figure 5A and 5B). Furthermore, in the absence of angiogenic stimuli, siRNA against TXNIP significantly stimulated thioredoxin activity ($P<0.0001$ versus control; Figure 6A) and strongly stimulated HMVEC migration (Figure 6B, $P<0.0001$ versus control). These studies indicate that inhibition of TXNIP by cholinergic or growth factor activation promotes endothelial cell migration, via derepression of thioredoxin activity. Furthermore, VEGF- or bFGF-mediated regulation of TXNIP expression is dependent on activation of nAChR (Figure 4A).

Discussion

We report a cholinergic contribution to growth factor-induced endothelial cell migration. The salient observations are that: (1) activation of nAChR induces EC migration similar in magnitude to that observed for bFGF or VEGF; (2) antagonism of nAChR markedly attenuates the migragenic effects of bFGF or VEGF on ECs; (3) the nAChR-dependent effects of bFGF and VEGF on EC migration are due, in large part, to activation of the α7-nAChR isoform; (4) nAChR activation induces a transcriptional profile that has many overlapping features to those induced by bFGF or VEGF, particularly for genes involved in EC migration; (5) downregulation of TXNIP with subsequent induction of thioredoxin activity is shown to be important to the migragenic effects exerted by each of the stimuli; (6) antagonism of the nAChR abrogates VEGF- or bFGF-mediated regulation of TXNIP expression. In toto, our findings identify a novel role for the nicotinic cholinergic pathway in growth factor-mediated EC migration, a critical event in angiogenesis.

Previous studies have demonstrated that ECs synthesize, store, and release acetylcholine[16] and express functional nAChRs.[2] Increasing evidence suggests that such nonneuronal nAChRs are involved in the regulation of vital cell functions, such as mitosis, differentiation, organization of the cytoskeleton, cell–cell contact, locomotion, and migration.[17] Thus, acetylcholine, originally identified as a neurotransmitter, may function as an autocrine factor that modulates migration of endothelial cells. We and others have previously shown that exogenous nicotine, at pathophysiologically relevant concentrations, promotes angiogenesis in a number of in vivo settings, including inflammation, wound healing, ischemia, tumor, and atherosclerosis.[4,7,18] Furthermore, inhibition of nAChR, in the absence of exogenous nicotine, reduces the angiogenic response in vitro and in vivo, indicating that there exists an endogenous cholinergic pathway for angiogenesis.[5] In contrast, recent work has shown that VEGF and FGF, originally identified as angiogenic growth factors, exert neurotrophic effects and promote neurogenesis.[19,20] These and other data suggest that there may be interdependence between "vascular" and "neuronal" factors and processes.

In this study, we found that nicotine induced dose-dependent nAChR-mediated EC migration which was maximal at concentrations consistent with those found in moderate smokers (10^{-8} mol/L). Surprisingly, coadministration of nAChR antagonists, hexamethonium, or mecamylamine, significantly attenuated the migragenic response of ECs to both VEGF and bFGF. Although several nAChR isoforms exist, we have previously identified a principal role for the α7-nAChR isoform in nAChR-mediated

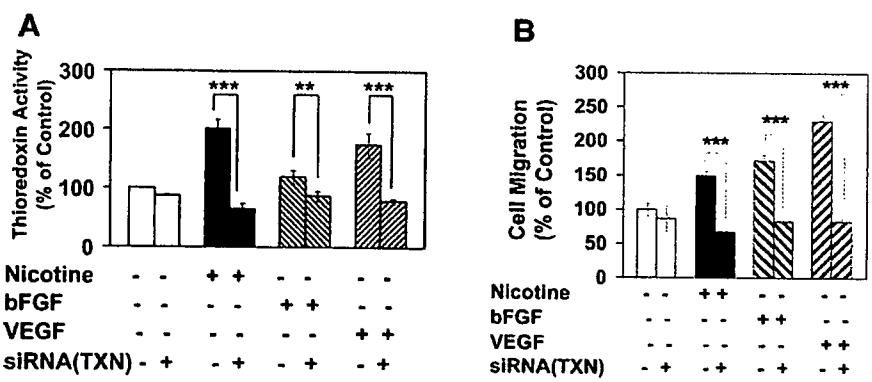

Figure 5. Effects of gene knockdown of thioredoxin by small interference RNA (siRNA) on induction of thioredoxin activity in human microvascular endothelial cells (HMVECs) by nicotine (10^{-8} mol/L), VEGF(10 ng/mL), or bFGF (10 ng/mL) (A) and HMVEC migration induced by nicotine, VEGF, or bFGF (B). Scrambled (randomly arranged) siRNA had no effect on thioredoxin activity or HMVEC migration (data not shown). Values for thioredoxin activity and migration are expressed as a percentage of control (vehicle-treated cells). TXN indicates thioredoxin. $^{**}P$=0.01; $^{***}P<0.001$.

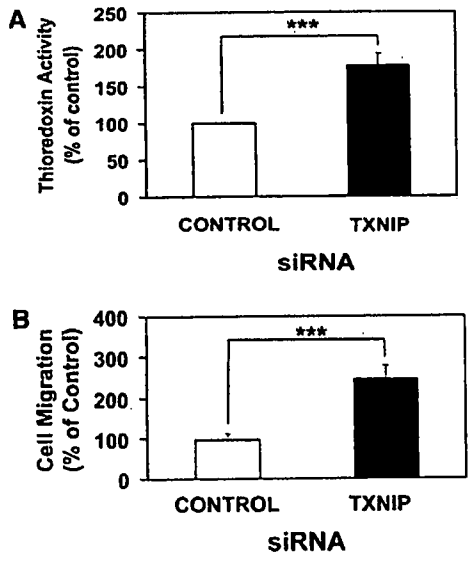

Figure 6. Effects of gene knockdown of thioredoxin interacting protein (TXNIP) by small interference RNA (siRNA) on thioredoxin activity (A) and human microvascular endothelial cell (HMVEC) migration (B). Scrambled (randomly arranged) siRNA had no effect on thioredoxin activity or HMVEC migration (data not shown). Values for thioredoxin activity and migration are expressed as a percentage of control (vehicle-treated cells). ***$P<0.0001$.

angiogenesis in vitro and in vivo.[5] Consistent with these findings, we now find that VEGF and bFGF both induced changes in ∝7-nAChR expression consistent with activation of ∝7-nAChR. Moreover, the ∝7-nAChR selective antagonist, ∝-bungarotoxin, attenuated VEGF and bFGF-induced EC migration to a similar extent as for the nonselective antagonists, hexamethonium, and mecamylamine. These latter findings suggest that nAChR-dependent pathways, particularly via ∝7-nAChR activation, are involved in the modulation of growth factor–induced EC migration.

To study the relationship between nicotine and angiogenic growth factors at a genomic level, microarray analysis was performed after HMVEC exposure to nicotine, VEGF, or bFGF. By hierarchical clustering, we found that each stimulus induced distinct but overlapping transcriptional responses, with concordant gene expression being concentrated within six largely functionally coherent gene clusters. A major functional theme among concordantly expressed genes was the coregulation of cell motility-related processes by all three angiogens. In particular, a "migration" cluster of concordantly activated genes was strongly enriched for genes involved in cytokinetic-related processes such as the Rho GTPase cell motility pathways, integrin binding, cell cycle regulation, and NF-κB activation. Our findings with regard to activation of Rho GTPase pathways by VEGF and bFGF are consistent with previous studies[21] and reinforce the central role of Rho-related regulation of actomyosin cytoskeletal organization EC migration during angiogenesis. We previously demonstrated that nAChR-dependent endothelial tube formation in vitro is dependent on NF-κB activation.[5] The migration cluster included two genes associated with NF-κB activation: BCL10, an important activator of NF-κB downstream of protein kinase C, and CASP8AP2 (aka FLASH), which coordinates downstream NF-κB activity via a TRAF2-dependent pathway.[22] In addition, many genes within the migration cluster have been implicated in oncogenesis (MDM2, ADAM9, BCL10, etc), a finding pathogenetically consistent with the role of angiogenesis in cancer.

The majority of concordantly regulated genes revealed by our microarray analyses have not been previously associated with angiogenesis. These include the p53 inhibitor MDM2 (activated by all three stimuli) and TXNIP, C-C chemokines, and metallothioneins (repressed by all three stimuli). These concordant transcriptional profiles provide further evidence for a cholinergic component of the angiogenic pathways. For example, our findings of coinduction of FLT1 by all three stimuli, and of nAChR subunit induction by VEGF are consistent with interaction between the signaling pathways.

Of the coregulated genes identified by hierarchical clustering, we focused our attention on TXNIP. Originally identified in HL-60 leukemia cells treated with 1,25 dihydroxyvitamin D_3 (and previously known as Vitamin D_3 upregulated protein 1), TXNIP is an endogenous inhibitor of the ubiquitous redox protein thioredoxin.[12] Thioredoxin, a major redox regulator of protein function and signaling via thiol redox control, has been implicated in the regulation of cellular responses to oxidative stress and apoptosis.[23] Thioredoxin selectively regulates the activity of DNA-binding proteins; for example, two transcription factors concordantly regulated by the three stimuli, NF-κB, and p53, require thioredoxin reduction for stimulation of DNA binding.[23,24] Increasing evidence implicates TXNIP and thioredoxin in tumorigenesis. Thioredoxin expression is increased in several human primary cancers, whereas TXNIP is strongly downregulated in human tumor tissues.[13,25] Inhibition of thioredoxin signaling with experimental antitumor agents such as PX-12 (1-methylpropyl 2-imidazolyl disulfide) and pleurotin reduces tumor cell production of HIF-1α and VEGF in vitro and inhibits tumor angiogenesis in vivo.[26] We hypothesized that repression of TXNIP may play a role in mediating growth factor–mediated EC migration.

In the present study, we found that nicotine, VEGF, and bFGF stimulated thioredoxin activity—a finding consistent with their common suppression of TXNIP. Gene knockdown of thioredoxin by siRNA reversed the effect of growth factor stimulation and abrogated the effect of nicotine, VEGF, or bFGF on EC migration. These findings are consistent with a critical role for thioredoxin in mediating growth factor–induced EC migration. Interestingly, the increase in thioredoxin activty induced by each of the three stimuli could be blocked by nAChR antagonism. Finally, gene knockdown of TXNIP alone, without addition of growth factors, induced EC migration. Our findings indicate that TXNIP, by regulating of thioredoxin activity, may play an important role in angiogenesis mediated by growth factor receptors or nAChRs. The mechanism whereby thioredoxin mediates EC migration is poorly understood but may involve stimulation of hypoxia-inducible factor-1α (HIF-1α), a transcription factor that plays a central role in mediating the angiogenic response to hypoxia. Overexpression of thioredoxin in a variety of malignant cells has been shown to induce HIF-1α expression and VEGF production.[27] Induction of HIF-1α in human endothelial cells upregulates the expression of multiple angiogenic factors including the angiopoietins which are potent stimulators of cell migration via Tie-2 signal transduction pathways.[28] Moreover, as cellular redox state is an important determinant of Rho

GTPase activity, it is possible that thioredoxin may play a role in Rho-mediated cytoskeletal remodelling during cell migration.[29]

In summary, our data show that activation of nicotinic acetylcholine receptors (nAChRs) induces endothelial cell migration. Furthermore, growth factor (VEGF and bFGF)–induced endothelial cell migration involves nAChR activation. By transcriptional profiling we have identified convergent genomic responses of ECs to nicotine, VEGF, and bFGF. Identification of concordantly regulated genes may provide novel insights into molecular processes mediating EC migration and angiogenesis. Indeed, using this approach we found that TXNIP, by regulating thioredoxin activity, is centrally involved in nAChR-mediated EC migration. Our studies provide evidence for a cholinergic contribution to growth factor-induced EC migration. The nAChRs may play an important role in growth factor-induced angiogenesis, and thus may be a target for therapeutic modulation in disorders of pathological or insufficient angiogenesis.

Acknowledgments

We thank Mary Gerritsen, PhD, and Ken Kengatharan, PhD for scientific and editorial comments.

Sources of Funding

Akiko Ishii-Watabe is supported by the Japanese Health Sciences Foundation. Martin K.C. Ng is supported by the National Health and Medical Research Council of Australia. This study was supported by grants from the National Institutes of Health (R01 HL-63685; RO1 HL-75774; R01 CA098303 and P01 AG18784; and PO1AI50153); Philip Morris USA Inc; and the Tobacco Related Disease Research Program (11RT-0147).

Disclosures

Dr Cooke holds equity in Athenagen Inc, which has licensed Stanford University patents for the use of nAChR agonists and antagonists for disorders of angiogenesis. Dr Cooke is an inventor on these patents, and receives royalties from the licenses. A patent is being filed based upon the intellectual property described in this manuscript that may benefit J.P.C., M.K.C.N., E.C., and J.W.

References

1. Lindstrom J. Nicotinic acetylcholine receptors in health and disease. *Mol Neurobiol.* 1997;15:193–222.
2. Macklin KD, Maus AD, Pereira EF, Albuquerque EX, Conti-Fine BM. Human vascular endothelial cells express functional nicotinic acetylcholine receptors. *J Pharmacol Exp Ther.* 1998;287:435–439.
3. Parnavelas JG, Kelly W, Burnstock G. Ultrastructural localization of choline acetyltransferase in vascular endothelial cells in rat brain. *Nature.* 1985;316:724–725.
4. Heeschen C, Jang JJ, Weis M, Pathak A, Kaji S, Hu RS, Tsao PS, Johnson FL, Cooke JP. Nicotine stimulates angiogenesis and promotes tumor growth and atherosclerosis. *Nat Med.* 2001;7:833–839.
5. Heeschen C, Weis M, Aicher A, Dimmeler S, Cooke JP. A novel angiogenic pathway mediated by non-neuronal nicotinic acetylcholine receptors. *J Clin Invest.* 2002;110:527–536.
6. Zhu BQ, Heeschen C, Sievers RE, Karliner JS, Parmley WW, Glantz SA, Cooke JP. Second hand smoke stimulates tumor angiogenesis and growth. *Cancer Cell.* 2003;4:191–196.
7. Jacobi J, Jang J, Sundram U, Dayoub H, Fajardo LF, Cooke JP. Nicotine accelerates angiogenesis and wound healing in genetically diabetic mice. *Am J Pathol.* 2002;161:97–104.
8. Eisen MB, Spellman PT, Brown PO, Botstein D. Cluster analysis and display of genome-wide expression patterns. *Proc Natl Acad Sci U S A.* 1998;95:14863–14868.
9. Ridley A, Schwartz M, Burridge K, Firtel R, Ginsberg M, Borisy G, Parsons J, Horwitz A. Cell migration: integrating signals from front to back. *Science.* 2003;302:1704–1709.
10. Kiosses W, Daniels R, Otey C, Bokoch G, Schwartz M. A role for p21-activated kinase in endothelial cell migration. *J Cell Biol.* 1999;147:831–844.
11. Henkel G, Krebs B. Metallothioneins: zinc, cadmium, mercury, and copper thiolates and selenolates mimicking protein active site features - structural aspects and biological implications. *Chem Rev.* 2004;104:801–824.
12. Nishiyama A, Matsui M, Iwata S, Hirota K, Masutani H, Nakamura H, Takagi Y, Sono H, Gon Y, Yodoi J. Identification of thioredoxin-binding protein-2/vitamin D(3) up-regulated protein 1 as a negative regulator of thioredoxin function and expression. *J Biol Chem.* 1999;274:21645–21650.
13. Baker A, Payne CM, Briehl MM, Powis G. Thioredoxin, a gene found overexpressed in human cancer, inhibits apoptosis *in vitro* and *in vivo*. *Cancer Res.* 1997;57:5162–5167.
14. Yoshioka J, Schulze PC, Cupesi M, Sylvan JD, MacGillivray C, Gannon J, Huang H, Lee RT. Thioredoxin-interacting protein controls cardiac hypertrophy through regulation of thioredoxin activity. *Circulation.* 2004;109:2581–2586.
15. Wang YG, De Keulenaer GW, Lee RT. Vitamin D(3)-up-regulated protein-1 is a stress-responsive gene that regulates cardiomyocyte viability through interaction with thioredoxin. *J Biol Chem.* 2002;277:26496–26500.
16. Milner P, Kirkpatrick KA, Ralevic V, Toothill V, Pearson J, Burnstock G. Endothelial cells cultured from human umbilical vein release ATP, substance P and acetylcholine in response to increased flow. *Proc Biol Sci.* 1990;241:245–248.
17. Wessler I, Kirkpatrick CJ, Racke K. The cholinergic 'pitfall': acetylcholine, a universal cell molecule in biological systems, including humans. *Clin Exp Pharmacol Physiol.* 1999;26:198–205.
18. Natori T, Sata M, Washida M, Hirata Y, Nagai R, Makuuchi M. Nicotine enhances neovascularization and promotes tumor growth. *Mol Cells.* 2003;16:143–146.
19. Jin K, Zhu Y, Sun Y, Mao XO, Xie L, Greenberg DA. Vascular endothelial growth factor (VEGF) stimulates neurogenesis in vitro and in vivo. *Proc Natl Acad Sci U S A.* 2002;99:11946–11950.
20. Yoshimura S, Takagi Y, Harada J, Teramoto T, Thomas SS, Waeber C, Bakowska JC, Breakefield XO, Moskowitz MA. FGF-2 regulation of neurogenesis in adult hippocampus after brain injury. *Proc Natl Acad Sci U S A.* 2001;10:5874–5879.
21. Soga N, Namba N, McAllister S, Cornelius L, Teitelbaum S, Dowdy S, Kawamura J, Hruska K. Rho family GTPases regulate VEGF-stimulated endothelial cell motility. *Exp Cell Res.* 2001;269:73–87.
22. Choi Y, Kim K, Kim H, Hong G, Kwon Y, Chung C, Park Y, Shen Z, Kim B, Lee S, Jung Y. FLASH coordinates NF-kappa B activity via TRAF2. *J Biol Chem.* 2001;276:25073–25077.
23. Yamawaki H, Haendeler J, Berk BC. Thioredoxin. A key regulator of cardiovascular homeostasis. *Circ Res.* 2003;93:1029–1033.
24. Ueno M, Masutani H, Arai RJ, Yamauchi A, Hirota K, Sakai T, Inamoto T, Yamaoka Y, Yodoi J, Nikaido T. Thioredoxin-dependent redox regulation of p53-mediated p21 activation. *J Biol Chem.* 1999;274:35809–35815.
25. Kakolyris S, Giatromanolaki A, Koukourakis M, Powis G, Souglakos J, Sivridis E, Georgoulias V, Gatter KC, Harris AL. Thioredoxin expression is associated with lymph node status and prognosis in early operable non-small cell lung cancer. *Clin Cancer Res.* 2001;7:3087–3091.
26. Welsh SJ, Williams RR, Birmingham A, Newman DJ, Kirkpatrick DL, Powis G. The thioredoxin redox inhibitors 1-methylpropyl 2-imidazolyl disulfide and pleurotin inhibit hypoxia-induced factor 1alpha and vascular endothelial growth factor formation. *Mol Cancer Ther.* 2003;2:235–243.
27. Welsh SJ, Bellamy WT, Briehl MM, Powis G. The redox protein thioredoxin-1 (Trx-1) increases hypoxia-inducible factor 1alpha protein expression: Trx-1 overexpression results in increased vascular endothelial growth factor production and enhanced tumor angiogenesis. *Cancer Res.* 2002;62:5089–5095.
28. Yamakawa M, Liu LX, Date T, Belanger AJ, Vincent KA, Akita GY, Kuriyama T, Cheng SH, Gregory RJ, Jiang C. Hypoxia-inducible factor-1 mediates activation of cultured vascular endothelial cells by inducing multiple angiogenic factors. *Circ Res.* 2003;93:664–673.
29. Nimnual AS, Taylor LJ, Bar-Sagi D. Redox-dependent downregulation of Rho by Rac. *Nat Cell Biol.* 2003;5:236–241.

Gene Therapy (2007), 1–8

www.nature.com/gt

ORIGINAL ARTICLE

Downregulation of human CD46 by adenovirus serotype 35 vectors

F Sakurai[1], K Akitomo[1], K Kawabata[1], T Hayakawa[2] and H Mizuguchi[1,3]

[1]Laboratory of Gene Transfer and Regulation, National Institute of Biomedical Innovation, Osaka, Japan; [2]Pharmaceuticals and Medical Devices Agency, Tokyo, Japan and [3]Graduate School of Pharmaceutical Sciences, Osaka University, Osaka, Japan

Human CD46 (membrane cofactor protein), which serves as a receptor for a variety of pathogens, including strains of measles virus, human herpesvirus type 6 and Neisseria, *is rapidly downregulated from the cell surface following infection by these pathogens. Here, we report that replication-incompetent adenovirus (Ad) serotype 35 (Ad35) vectors, which belong to subgroup B and recognize human CD46 as a receptor, downregulate CD46 following infection. A decline in the surface expression of CD46 in human peripheral blood mononuclear cells was detectable 6 h after infection, and reached maximum (72%) 12 h after infection. Ad35 vector-induced downregulation of surface CD46 levels gradually recovered after the removal of Ad35 vectors, however, complete recovery of CD46 expression was not observed even at 96 h after removal. The surface expression of CD46 was also reduced after incubation with fiber-substituted Ad serotype 5 (Ad5) vectors bearing Ad35 fiber proteins, ultraviolet-irradiated Ad35, vectors and recombinant Ad35 fiber knob proteins; in contrast, conventional Ad5 vectors did not induce surface CD46 downregulation, suggesting that the fiber knob protein of Ad35 plays a crucial role in the downregulation of surface CD46 density. These results have important implications for gene therapy using CD46-utilizing Ad vectors and for the pathogenesis of Ads that interact with CD46.*
Gene Therapy advance online publication, 22 March 2007; doi:10.1038/sj.gt.3302946

Keywords: *adenovirus serotype 35 vector; CD46; downregulation; fiber knob; peripheral blood mononuclear cells*

Introduction

Human CD46 is a transmembrane glycoprotein, which is ubiquitously expressed in most or all human nucleated cells. CD46 functions as a regulator of complement activation, whose normal function is to protect the host from autologous complement attack, by binding complement components C3b and C4b and facilitating their cleavage by factor I.[1,2] In addition to these functions, CD46 serves as a receptor for several pathogens, including strains of measles virus (MV),[3] human herpesvirus type 6 (HHV6),[4] group A *streptococci*[5] and *Neisseria*.[6] Among these pathogens, infection by certain strains of MV,[7,8] HHV6[4] and *Neisseria gonorrhoeae*[9] has been shown to cause CD46 downregulation from the cell surface. The detailed mechanisms of surface CD46 downregulation upon infection by these pathogens remain to be elucidated, however, the decrease in the surface density of CD46 renders the cells more susceptible to lysis by complements, as demonstrated *in vitro*,[10] and may contribute to the attenuation of these pathogens by rapid clearing of infected cells.

Recently, it has been demonstrated that CD46 also acts as a receptor for the majority of subgroup B adenoviruses (Ads), including Ad serotypes 11 (Ad11) and 35 (Ad35).[11,12] The fiber knob domain of Ad11 or Ad35 binds to short consensus repeats (SCRs) 1 and/or 2 in CD46 for infection.[13–15] Furthermore, Ad35 competes for binding to CD46 with the MV hemagglutinin (MVH) protein,[14] which is responsible for both the attachment of MV to CD46[16] and downregulation of surface CD46 expression levels.[17] These findings led us to hypothesize that CD46 is downregulated following infection by subgroup B Ads, as occurs in the case of MV. On the other hand, subgroup B Ad11 and Ad35 are considered to be an attractive framework for gene transfer vectors for the following reasons. First, Ad11 and Ad35 are known to be rarely neutralized by human sera.[18] Second, Ad11 and Ad35 exhibit a broad tropism including cells expressing no or low levels of coxsackievirus and adenovirus receptor (CAR), which is a receptor for Ads belonging to subgroups A, C, D, E and F.[19] Several groups (including the authors) have developed replication-incompetent Ad vectors composed of subgroup B Ads[20–24] or fiber-substituted Ad serotype 5 (Ad5) vectors containing subgroup B Ad fibers,[25–28] and have demonstrated that these types of Ad vectors efficiently transduce a variety of human cells, including cells refractory to conventional Ad5 vectors. If surface CD46 downregulation occurs following transduction with CD46-utilizing Ad vectors, unexpected side effects might occur such as complement-mediated cell lysis of successfully transduced cells, which leads to clearance of the transduced cells.

In the present study, we examined replication-incompetent Ad35 vector-induced downregulation of surface

Correspondence: Dr H Mizuguchi, Laboratory of Gene Transfer and Regulation, National Institute of Biomedical Innovation, 7-6-8 Asagi, Saito, Ibaragi City, Osaka 567-0085, Japan.
E-mail: mizuguch@nibio.go.jp
Received 24 September 2006; revised 7 February 2007; accepted 7 February 2007

CD46 expression. We found that transduction with Ad35 vectors significantly downregulated CD46 expression from the cell surface in a dose-dependent and cell type-specific manner. Ad35 vector-mediated downregulation of surface CD46 was found to occur in leukemia cells, whereas nonleukemia cells did not exhibit any decline in surface CD46 expression following Ad35 vector infection. To the best of our knowledge, this is the first report characterizing subgroup B Ad-mediated downregulation of surface CD46.

Results

Infection with Ad35 vectors causes downregulation of surface CD46 expression

To determine whether infection with Ad35 vectors results in modulation of surface CD46 expression, human peripheral blood mononuclear cells (PBMCs) were incubated with the Ad35 vector expressing green fluorescence protein (GFP) (Ad35GFP) at 10 000 vector particle (VP)/cell and subjected to flow cytometric analysis at various time points. This analysis demonstrated that the surface expression levels of CD46 in PBMCs gradually decreased during exposure to Ad35GFP (Figure 1a). The significant decrease in CD46 was detectable 6 h after infection and reached maximum 12 h after infection (72% downregulation). Furthermore, the downregulation of surface CD46 by Ad35 vectors was found to be dose dependent (Figure 1b). PBMCs infected at 1250 VP/cell showed significantly reduced levels of CD46 expression (44% downregulation), and 71% downregulation of surface CD46 expression was induced at 20 000 VP/cell. These results indicate that infection with Ad35 vectors downregulates surface CD46 expression, as happens in the cases of MV[7,8] and HHV6.[4] The viability of PBMCs was not significantly affected by Ad35 vector infection (data not shown).

Next, in order to examine whether B cells ($CD19^+$ cells) and T cells ($CD3^+$ cells) in PBMCs show a reduction in surface CD46 levels after infection with Ad35 vectors, PBMCs were simultaneously stained with anti-human CD46 and anti-human CD19 or anti-human CD3 antibodies, and were subsequently subjected to flow cytometric analysis. Surface CD46 downregulation was found in both B cells and T cells after Ad35 vector infection, but the levels of the downregulation in these cells were lower than those of whole PBMCs (Figure 1c). Surface CD46 expression in T cells was more largely reduced than that in B cells. We also investigated seven additional human cells (Molt-4, KG-1a, K562, U937, A549, HeLa and human bone marrow-derived $CD34^+$ cells) for Ad35 vector-induced downregulation of surface CD46 levels; the downregulation levels of surface CD46 were different among the cell types (Table 1). K562, U937, KG-1a and Molt-4 cells exhibited a decrease in CD46 expression following Ad35 vector infection (by 36% in K562 cells, 24% in U937 cells, 18% in KG-1a cells

Table 1 Downregulation of CD46 induced by Ad35 vectors in various types of cells

Cell type	*% CD46 downregulation*
Molt-4	55±5.7
KG-1a	18±2.6
K562	36±1.9
U937	24±8.6
A549	−10±8.0
HeLa	7.9±18
Human bone marrow-derived $CD34^+$ cells	−11±5.2

The cells were infected with Ad35L at 10 000 VP/cell. After incubation for 24 h, CD46 expression on the cell surface was determined by flow cytometry as described in Materials and methods. Values represent mean±s.d. of quadruplicate results from two similar experiments.

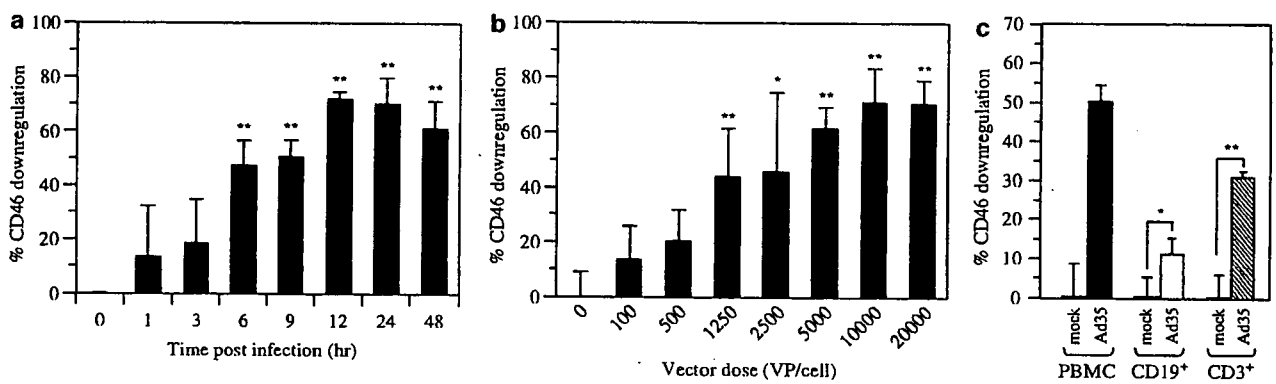

Figure 1 Downregulation of CD46 from the cell surface of PBMCs after infection by Ad35 vectors. (a) Time course of CD46 downregulation from the cell surface of PBMCs after infection with Ad35GFP. PBMCs were incubated with Ad35GFP at 10 000 VP/cell for up to 48 h. Cells were harvested at the indicated time points and stained with anti-human CD46 antibodies after fixation. The expression levels of CD46 on the cell surface were determined by flow cytometry. (b) Dose-dependent downregulation of surface CD46 after infection with Ad35 vectors. PBMCs were infected with Ad35GFP at the indicated vector doses for 24 h. After incubation for 24 h, PBMCs were harvested and CD46 expression levels were determined by flow cytometry. (c) Surface CD46 downregulation in B cells and T cells after infection with Ad35 vectors. PBMCs were infected with Ad35L at 10 000 VP/cell. After incubation for 24 h, PBMCs were harvested and stained with both anti-human CD46 antibody and anti-human CD19 or anti-human CD3 antibody. Subsequently, the cells were subjected to flow cytometric analysis. The asterisks indicate the level of significance ($P<0.005$ (double asterisk), $P<0.05$, (single asterisk)). Values represent mean±s.d. of quadruplicate results from one of at least two similar experiments.

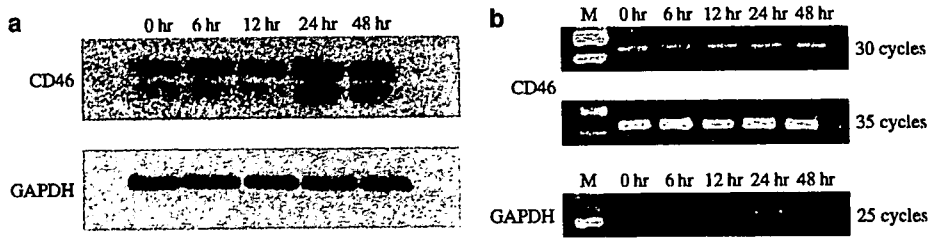

Figure 2 Total cellular protein levels and mRNA levels of CD46 following infection by Ad35 vectors. (a) Western blotting analysis for the total cellular protein levels of CD46 in PBMCs infected with Ad35GFP. PBMCs were incubated with Ad35GFP at 10 000 VP/cell for up to 48 h. Cells collected at the indicated time points were lysed and quantified by immunoblotting for their total cellular amounts of CD46. GAPDH bands served as an internal control for equal total protein loading. This result was representative of three independent experiments. (b) Semiquantitative RT-PCR analysis of CD46 in PBMCs infected with Ad35GFP. PBMCs were infected with Ad35GFP as described for Western blotting analysis in Materials and methods. Total RNA was prepared from PBMCs following incubation with Ad35GFP, and RT-PCR was then performed as described in Materials and methods. Lane M: 100-bp ladder. These results were representative of at least two independent experiments.

and 55% in Molt-4 cells), whereas CD46 expression was reduced not at all or only slightly in nonleukemia cells (A549, HeLa and bone marrow CD34$^+$ cells). Indeed, a slight increase in CD46 expression on the cell surface was found in A549 and CD34$^+$ cells following Ad35 vector infection.

Total protein levels and mRNA levels of CD46 are not reduced following Ad35 vector infection

To examine the mechanism of Ad35 vector-induced downregulation of surface CD46, Western blotting and semiquantitative reverse transcriptase-polymerase chain reaction (RT-PCR) analysis for CD46 expression were performed. Western blotting analysis using total cellular lysates demonstrated that the total cellular levels of CD46 were not reduced, but rather seemed to slightly increase, during 48 h of exposure to Ad35GFP (Figure 2a), suggesting that CD46 may be internalized after infection by Ad35 vectors without intracellular degradation, as in the case of MV.[7] In addition, infection by Ad35GFP did not decrease the mRNA levels of CD46 (Figure 2b). These results indicate that infection by Ad35 vectors does not downregulate the transcription of the *CD46* gene.

Fiber knob proteins of subgroup B Ads play a crucial role in the decrease in surface CD46 expression

To investigate which parts of Ad35 are involved in the downregulation of surface CD46 levels, PBMCs were incubated with conventional Ad5 vectors, fiber-substituted Ad5 vectors displaying the Ad35 fiber shaft and knob, and ultraviolet (UV)- or heat-inactivated Ad35 vectors at 10 000 VP/cell for 24 h. The conventional Ad5 vectors expressing GFP, Ad5GFP, which utilizes CAR for infection, did not downregulate CD46, whereas infection by the Ad5F35 vector expressing GFP, Ad5F35GFP, which recognizes CD46 for infection, significantly reduced surface CD46 expression by 72% (Figure 3a). UV-inactivated Ad35GFP also induced the downregulation of surface CD46 by 62% following infection, which was a level similar to that of surface CD46 downregulation induced by Ad35GFP. However, heat-inactivated Ad35GFP produced a lower level of surface CD46 downregulation than UV-inactivated Ad35GFP. This low level of CD46 downregulation by heat-inactivated Ad35GFP

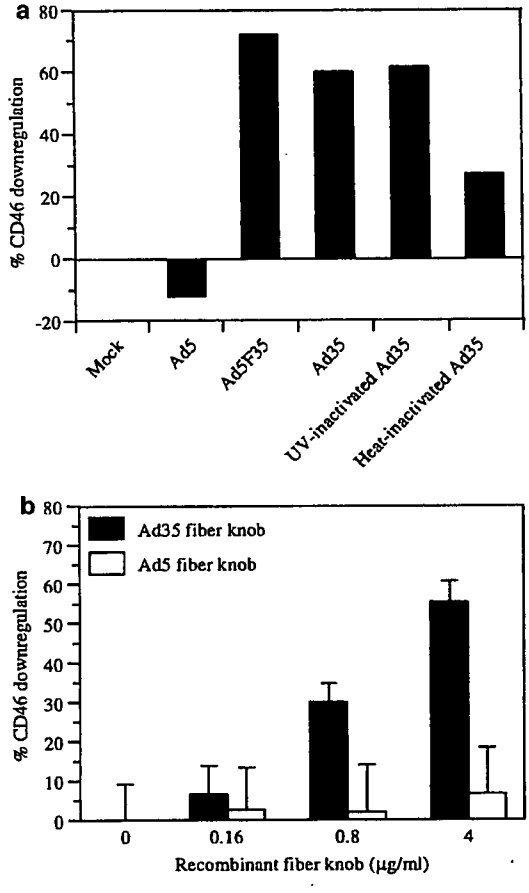

Figure 3 Role of Ad35 fiber knob protein on downregulation of surface CD46. (a) Downregulation of surface CD46 expression induced by various types of Ad vectors. PBMCs were incubated with Ad5GFP, Ad5F35GFP, Ad35GFP, UV-inactivated Ad35GFP or heat-inactivated Ad35GFP at 10 000 VP/cell for 24 h. After incubation, the cells were subjected to flow cytometric analysis to determine the level of CD46 expression. Values represent the mean of duplicate results from one of three similar experiments. (b) Downregulation of surface CD46 expression induced by Ad35 fiber knob protein. PBMCs were incubated with Ad5 or Ad35 fiber proteins at the indicated concentrations. After incubation for 24 h, the cells were subjected to flow cytometric analysis for the measurement of surface CD46 levels. Values represent the mean of quadruplicate results from one of three similar experiments.

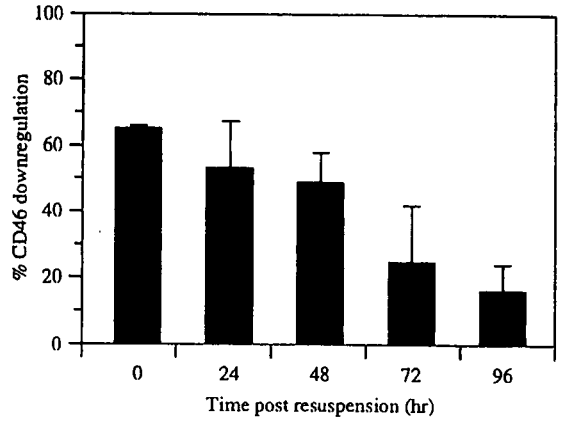

Figure 4 Recovery of surface CD46 expression after Ad35 vector-mediated downregulation. PBMCs were infected with Ad35GFP at 10 000 VP/cell for 24 h. After a 24-h infection, PBMCs were washed twice to remove the Ad35GFP, and resuspended and incubated in fresh medium. After incubation, cells were harvested at the indicated time points and CD46 expression was measured by flow cytometry. Values represent mean±s.d. of quadruplicate results from one of two similar experiments.

would be due to the thermal denaturation of fiber proteins in Ad35GFP.

Next, PBMCs were incubated with recombinant Ad5 or Ad35 fiber knob proteins to further examine the role of Ad35 fiber protein in the downregulation of surface CD46 expression. Ad35 fiber knob proteins were found to downregulate the surface expression levels of CD46 in a dose-dependent manner, and maximal downregulation of surface CD46 was induced by 55% at 4 μg/ml (Figure 3b). In contrast, no significant reduction in surface CD46 levels was found after incubation with Ad5 fiber knob proteins. These results indicate that fiber knob proteins of Ad35 play a crucial role in the downregulation of surface levels of CD46.

Downregulated CD46 expression is not rapidly restored after the removal of Ad35 vectors

Next, we examined how long it takes to restore surface CD46 expression after Ad35 vector-induced downregulation. Downregulation of surface CD46 induced by Ad35GFP gradually recovered after resuspension, however, the recovery kinetics of CD46 expression after the removal of Ad35 vectors was much lower than the kinetics of Ad35 vector-induced decrease in the surface CD46 (Figure 4). CD46 expression was downregulated by 65% before resuspension, and surface CD46 expression remained reduced by 53 and 49% at 24 and 48 h after resuspension, respectively. Complete restoration of surface CD46 expression was not observed even at 96 h after resuspension, at which point 17% downregulation remained, thus, more than 96 h are required to restore completely surface CD46 expression after Ad35 vector-induced downregulation.

Discussion

Understanding the interaction between cellular receptors and viruses and subsequent events following the attachment of viruses to receptors is important to elucidate the tropism, infectivity and pathogenicity of viruses. Many previous studies have assessed the interaction between CD46 and CD46-utilizing pathogens, especially MV, and have demonstrated that infection by CD46-utilizing pathogens causes unique cellular events. For example, downregulation of CD46 from the cell surface occurs following infection by MV,[7,17] HHV6[4] or *Neisseria*.[9] Additionally, MV and HHV6 suppress interleukin (IL)-12 production in infected human monocytes.[29,30] However, subsequent cellular events following the interaction between human CD46 and subgroup B Ads have not yet been fully evaluated. In the present study, we have demonstrated the downregulation of human CD46 from the cell surface following infection by Ad35 vectors belonging to subgroup B.

MV-induced downregulation of surface CD46 has been the most thoroughly studied aspect of the effects of pathogens recognizing CD46. Nevertheless, the precise mechanisms of MV-induced downregulation of surface CD46 remain to be clarified; surface CD46 downregulation by MV exhibits similar properties to that induced by Ad35 vectors. First, surface expression levels of CD46 are reduced, whereas the total cellular protein levels of CD46 are not significantly decreased after infection,[7] as demonstrated by Western blotting analysis (Figure 2a). These results suggest that CD46 may be internalized without degradation following infection by MV or Ad35. Second, the protein components, which bind to CD46 in the virion, MVH proteins and fiber knob proteins of Ad35, are involved with surface CD46 downregulation. Previous studies indicate that direct protein–protein contact between CD46 and MVH proteins is necessary for the MV-induced downregulation of surface CD46 levels.[31,32] The present data in Figure 3 indicate that fiber knob proteins of Ad35 play a crucial role in the reduction in surface CD46 expression. These common properties suggest that Ad35 might downregulate the surface expression levels of CD46 through a mechanism similar to the one that acts in the case of MV. This hypothesis is further supported by previous findings that both the MVH and fiber knob proteins of Ad35 recognize the domains within SCR1 and 2 of CD46.[13–15,33,34]

However, the Ad35 vector-mediated modulation of CD46 expression in nonleukemia cells differed from that induced by MVH protein: Ad35 vectors did not produce any decline in CD46 expression in the nonleukemia cells used in the present study (HeLa, A549 and human bone marrow-derived CD34$^+$ cells). We have also demonstrated that surface CD46 expression was not decreased following Ad35 vector infection in Chinese hamster ovary (CHO) transformants expressing CD46[15] (data not shown), however, the MVH protein downregulated CD46 expression in HeLa cells[31] and in CHO transformants stably expressing CD46.[35] These findings suggest that cellular events following the binding of Ad35 vectors to CD46 would be somewhat different from those induced by MV in nonleukemia cells.

Downregulation of surface CD46 levels by Ad35 vectors seems inefficient compared with that induced by MV. An approximately 24% reduction in CD46 expression was achieved in U937 cells 24 h following infection of Ad35L at 10 000 VP/cell, which is an approximate multiplicity of infection (MOI) of 50. In contrast, infection by MV strain Edmonston in U937 cells

induced a decline of about 70% in CD46 expression 12 h after infection even at an MOI of 5.[31] The lower levels of surface CD46 downregulation caused by replication-incompetent Ad35 vectors might be partly due to a lack of virus replication; a previous study suggests that newly synthesized MVH proteins in the infected cells further downregulate surface CD46 expression.[31]

Piliated *N. gonorrhoeae*, which also utilizes CD46 as a receptor, exhibits surface CD46 downregulation by the shedding of CD46.[9] The total levels of CD46 in the whole-cell lysates are reduced, and soluble CD46 is found in cell culture supernatants after exposure to piliated *N. gonorrhoeae*. It now remains unclear how piliated *N. gonorrhoeae* induces shedding of CD46. However, it is unlikely that Ad35 vector-induced shedding of CD46 occurs because total cellular levels of CD46 were not reduced following infection with Ad35 vectors (Figure 2a).

It is surprising that the downregulation of surface CD46 expression was not readily restored after the removal of Ad35 vectors because pulse-chase analysis of CD46 showed that matured forms of CD46 are synthesized within 1 h.[36] This raises the question of why newly synthesized CD46 is not transported to the surface membrane in Ad35 vector-infected cells and where newly synthesized CD46 stays in the cells. Further studies are necessary to address these questions.

Previous studies have demonstrated the increased susceptibility of cells to complement-mediated lysis as a result of surface CD46 downregulation,[10,31] however, we found no apparent lysis of PBMCs *in vitro* by complements following Ad35 vector infection (data not shown). It is now unclear why the complement-mediated cell lysis did not occur in cells showing CD46 downregulation by Ad35 vectors. One possible explanation is that the decreased levels of surface CD46 by Ad35 vectors might be enough to block the complement-mediated cell lysis. Other complement regulatory proteins might compensate the reduction in surface CD46 levels. Although PBMCs showing the reduction in surface CD46 density did not exhibit an apparent increase in susceptibility to complement-mediated cell lysis *in vitro*, this study suggests that we should exercise caution in the use of CD46-utilizing Ad vectors. The reduction in CD46 expression in cells transduced with CD46-utilizing Ad vectors might cause unexpected side effects after *in vivo* application. Recently, CD46 has been demonstrated to be involved in not only complement regulation but also various cellular functions, such as immune responses.[37,38] It is essential to further examine the influence of surface CD46 downregulation, including the fate of the transduced cells, before initiating clinical applications of CD46-utilizing Ad vectors. Additionally, the influence of surface CD46 downregulation *in vivo* should be evaluated in nonhuman primates; the use of human CD46-transgenic mice is not recommended because rodent CD46 expression is limited in testis, and other complement regulators, such as decay-accelerating factor, protect cells from complement attack in rodents.[39]

In summary, we have shown that infection by Ad35 vectors induces downregulation of human CD46 from the cell surface in a dose-dependent and cell type-specific manner. In addition to Ad35 vectors, fiber-substituted Ad5 vectors containing fiber proteins derived from Ad35 also downregulate the surface expression of CD46. Once the surface expression levels of CD46 have declined, CD46 expression is not readily restored after the removal of Ad35 vectors. The present study provides important clues for clarifying the pathogenicity of subgroup B Ad, and suggests caution in the use of Ad vectors recognizing CD46 for gene therapy.

Materials and methods

Cells

Human PBMCs (Cambrex Bio Science, Walkersville, MD, USA) were cultured in culture medium (Roswell Park Memorial Institute (RPMI)1640 supplemented with 10 mM *N*-2-hydroxyethylpiperazine-*N'*-2-ethanesulfonic acid, 1 mM sodium pyruvate, 0.1 mM nonessential amino acids, 4 mM L-glutamine, 10% fetal bovine serum (FBS)). HeLa cells (human cervix epitheloid carcinoma) were cultured with Dulbecco's modified Eagle's medium supplemented with 10% FBS. A549 cells (a human lung epithelial cell line) were cultured with F-12K medium supplemented with 10% FBS. K562 cells (human chronic myelogenous leukemia in blast crisis), U937 cells (a human lymphoma cell line), Molt-4 (a human T-cell leukemia cell line) and KG-1a cells (human bone marrow acute myelogenous leukemia) were cultured with RPMI1640 medium supplemented with 10% FBS. Human bone marrow-derived $CD34^+$ cells (Cambrex Bio Science) were cultured with StemSpan 2000 containing cytokine cocktail StemSpan CC100 (human Flt-3 ligand (100 ng/ml), human stem cell factor (100 ng/ml), human IL-3 (20 ng/ml) and human IL-6 (20 ng/ml)) (StemCell Technologies Inc., Vancouver, BC, Canada).

Ad vectors

Ad35 vectors containing a cytomegalovirus promoter-driven enhanced GFP expression cassette or a cytomegalovirus promoter-driven firefly luciferase expression cassette, Ad35GFP and Ad35L, respectively, were constructed by the improved *in vitro* ligation method described previously.[40] GFP-expressing conventional Ad5-based vectors, Ad5GFP and fiber-substituted Ad5-based vectors displaying the fiber knob and shaft of Ad35, Ad5F35GFP, were also constructed as described previously.[25,41] Determination of the virus particle titers of Ad vectors was accomplished following the method described by Maizel *et al*.[42] Ad35GFP was UV- and heat-inactivated by exposure to 254-nm radiation for 1 h, and by incubation at 48°C for 1 h, respectively. The efficiency of the inactivation was confirmed by comparing the transduction efficiencies of control and inactivated Ad35GFP.

Downregulation of surface CD46 by infection with Ad35 vectors

For the present time course study of the downregulation of surface CD46, PBMCs were seeded in a 96-well plate at 5.0×10^4 cells/well and incubated with Ad35GFP at 10 000 VP/cell. PBMCs were harvested at various time points and subjected to flow cytometric analyses as described below. For the study of the dose-dependent downregulation of surface CD46, PBMCs were infected with Ad35GFP at the indicated vector doses. After incubation for 24 h, the surface expression levels of CD46

were measured by flow cytometry. Analysis of the downregulation of surface CD46 levels in response to various types of Ad vectors was similarly performed. Ad35 vector-mediated decrease in the surface CD46 levels was also assessed in various types of human cells (Molt-4, KG-1a, K562, U937, A549, HeLa and human bone marrow-derived $CD34^+$ cells). Cells were seeded in a 24- or 96-well plate and infected with Ad35L at 10 000 VP/cell. After incubation for 24 h, CD46 expression levels were assessed by flow cytometry.

Ad35 fiber knob-mediated downregulation of surface CD46

Recombinant Ad35 fiber knob protein was constructed similarly to Ad5 fiber knob,[43] using Ad35 vector plasmid pAdMS4[44] and the following primers: forward, 5′-tcg aat tca cct tat gga ctg gaa taa acc c-3′ (*Eco*RI site is underlined); reverse, 5′-atg cgg ccg ctt agt tgt cgt ctt ctg taa tgt aag a-3′ (*Not*I site is underlined). Ad5 fiber knob protein was prepared previously.[43] PBMCs, which were seeded in a 96-well plate at 5.0×10^4 cells/well, were incubated with the Ad5 or Ad35 fiber knob at the indicated concentrations. Surface CD46 expression levels were examined 24 h after incubation by flow cytometry as described below.

Western blotting analysis for CD46 expression

PBMCs (5.0×10^5 cells) were seeded in a 24-well plate and infected with Ad35GFP at 10 000 VP/cell. They were then collected at the indicated time points, washed and treated with lysis buffer (25 mM Tris, 1% Triton X-100, 0.5% sodium deoxycholate, 5 mM ethylenediaminetetraacetic acid, 150 mM NaCl) containing a cocktail of protease inhibitors (Sigma, St Louis, MO, USA). The protein content in the cell lysates was measured with an assay kit from Bio-Rad (Hercules, CA, USA), using bovine serum albumin (BSA) as a standard. Protein samples (10 μg) were subjected to nonreducing sodium dodecyl sulfate-12.5% polyacrylamide gel electrophoresis, and the separated proteins were transferred to a nitrocellulose membrane. After blocking nonspecific binding, CD46 was detected with anti-CD46 rabbit serum (1:5000; kindly provided by Dr Tsukasa Seya, Hokkaido University, Japan), followed by incubation in the presence of horseradish peroxidase-labeled goat anti-rabbit second antibody (1:6000, Cell Signaling, Danvers, MA, USA). Signals on the membrane were visualized and analyzed as described previously.[40] To verify equal loading, the blots were stripped and probed with a rabbit anti-glyceraldehyde-3-phosphate dehydrogenase (GAPDH) (1:3000, Trevigen, Gaithersburg, MD, USA) followed by treatment with an horseradish peroxidase-conjugated goat anti-rabbit second antibody (1:5000, Cell Signaling).

RT-PCR analysis for CD46 expression

PBMCs were infected with Ad35GFP as performed in Western blotting analysis. After infection, the cells were collected at the indicated time points and total RNA was isolated from the cells using Isogen reagent (Nippon Gene, Tokyo, Japan). First-strand cDNA templates were synthesized as previously described,[43] and the templates were subjected to PCR amplification using sets of primers for human CD46[45] and GAPDH.[46] The cycling parameters were 30 s at 94°C, 30 s at 55°C and 30 s at 72°C for both CD46 and GAPDH. PCR products were separated by electrophoresis on a 2.0% agarose gel and visualized with ethidium bromide.

Recovery of CD46 expression from the Ad35 vector-mediated downregulation of surface CD46 expression

PBMCs seeded in a six-well plate were infected with Ad35GFP at 10 000 VP/cell. After a 24-h incubation, the cells were collected and washed twice to remove the Ad35GFP. The PBMCs were then resuspended in fresh culture medium, and subsequently cultured at 37°C PBMCs were harvested at the indicated time points and subjected to flow cytometric analysis to measure CD46 expression.

Flow cytometry

Cells were harvested, washed with FACS buffer (phosphate-buffered saline (PBS) containing 1% BSA and 0.01% sodium azide) and then fixed for 10 min with 3.2% paraformaldehyde-containing PBS. Cells were washed twice and incubated with anti-human CD46 antibody (J4.48, Immunotech, Marseilles, France; or E4.3, Pharmigen, San Diego, CA, USA) for 45 min on ice. Subsequently, the cells were washed and incubated with phycoerythrin (PE)-conjugated goat anti-mouse IgG second antibody (Pharmingen). After being washed thoroughly, stained cells were analyzed by FACSCalibur (Becton Dickinson, Tokyo, Japan) and CellQuest software (Becton Dickinson) to obtain the percentage of surface CD46 downregulation as follows: CD46 downregulation = 100−(100 × MFI of CD46 in infected cells)/(MFI of CD46 in uninfected cells), where MFI = mean fluorescence intensity.

For the simultaneous analysis of expression levels of CD46 and CD19 (B-cell marker) or CD3 (T cell marker), PBMCs were incubated with both fluorescein isothiocyanate (FITC)-labeled anti-human CD46 antibody (E4.3, Pharmingen) and PE-conjugated anti-human CD19 antibody (HIB19, Pharmingen) or allophycocyanin (APC)-labeled anti-human CD3 antibody (UCHT1, eBioscience, San Diego, CA, USA). After incubation for 45 min on ice, stained cells were subjected to flow cytometry analysis as described above.

Abbreviations

Ad, adenovirus; APC, allophycocyanin; BSA, bovine serum albumin; CAR, coxsackievirus and adenovirus receptor; FBS, fetal bovine serum; FITC, fluorescein isothiocyanate; GAPDH, glyceraldehyde-3-phosphate dehydrogenase; GFP, green fluorescence protein; HHV6, herpesvirus type 6; MV, measles virus; MVH, measles virus hemagglutinin; MFI, mean fluorescence intensity; MOI, multiplicity of infection; PBMCs, peripheral blood mononuclear cells; PBS, phosphate-buffered saline; RT-PCR, reverse transcriptase-polymerase chain reaction; SCRs, short consensus repeats; VP, vector particle; PE, phycoerythrin.

Acknowledgements

We thank Ms Naoko Funakoshi, Ms Tomomi Sasaki and Ms Noriko Tada for their technical assistance. We also

thank Dr Tsukasa Seya (Hokkaido University, Japan) for providing anti-CD46 rabbit serum. This work was supported by grants for Health and Labour Sciences Research from the Ministry of Health, Labour, and Welfare of Japan, and by Grants-in-Aid for Scientific Research on Priority Areas (B).

References

1 Liszewski MK, Post TW, Atkinson JP. Membrane cofactor protein (MCP or CD46): newest member of the regulators of complement activation gene cluster. *Annu Rev Immunol* 1991; 9: 431–455.
2 Seya T, Atkinson JP. Functional properties of membrane cofactor protein of complement. *Biochem J* 1989; 264: 581–588.
3 Dorig RE, Marcil A, Chopra A, Richardson CD. The human CD46 molecule is a receptor for measles virus (Edmonston strain). *Cell* 1993; 75: 295–305.
4 Santoro F, Kennedy PE, Locatelli G, Malnati MS, Berger EA, Lusso P. CD46 is a cellular receptor for human herpesvirus 6. *Cell* 1999; 99: 817–827.
5 Rezcallah MS, Hodges K, Gill DB, Atkinson JP, Wang B, Cleary PP. Engagement of CD46 and alpha5beta1 integrin by group A streptococci is required for efficient invasion of epithelial cells. *Cell Microbiol* 2005; 7: 645–653.
6 Kallstrom H, Liszewski MK, Atkinson JP, Jonsson AB. Membrane cofactor protein (MCP or CD46) is a cellular pilus receptor for pathogenic Neisseria. *Mol Microbiol* 1997; 25: 639–647.
7 Naniche D, Wild TF, Rabourdin-Combe C, Gerlier D. Measles virus haemagglutinin induces down-regulation of gp57/67, a molecule involved in virus binding. *J Gen Virol* 1993; 74 (Part 6): 1073–1079.
8 Schneider-Schaulies J, Dunster LM, Kobune F, Rima B, ter Meulen V. Differential downregulation of CD46 by measles virus strains. *J Virol* 1995; 69: 7257–7259.
9 Gill DB, Koomey M, Cannon JG, Atkinson JP. Down-regulation of CD46 by piliated *Neisseria gonorrhoeae*. *J Exp Med* 2003; 198: 1313–1322.
10 Schnorr JJ, Dunster LM, Nanan R, Schneider-Schaulies J, Schneider-Schaulies S, ter Meulen V. Measles virus-induced down-regulation of CD46 is associated with enhanced sensitivity to complement-mediated lysis of infected cells. *Eur J Immunol* 1995; 25: 976–984.
11 Gaggar A, Shayakhmetov DM, Lieber A. CD46 is a cellular receptor for group B adenoviruses. *Nat Med* 2003; 9: 1408–1412.
12 Segerman A, Atkinson JP, Marttila M, Dennerquist V, Wadell G, Arnberg N. Adenovirus type 11 uses CD46 as a cellular receptor. *J Virol* 2003; 77: 9183–9191.
13 Fleischli C, Verhaagh S, Havenga M, Sirena D, Schaffner W, Cattaneo R *et al*. The distal short consensus repeats 1 and 2 of the membrane cofactor protein CD46 and their distance from the cell membrane determine productive entry of species B adenovirus serotype 35. *J Virol* 2005; 79: 10013–10022.
14 Gaggar A, Shayakhmetov DM, Liszewski MK, Atkinson JP, Lieber A. Localization of regions in CD46 that interact with adenovirus. *J Virol* 2005; 79: 7503–7513.
15 Sakurai F, Murakami S, Kawabata K, Okada N, Yamamoto A, Seya T *et al*. The short consensus repeats 1 and 2, not the cytoplasmic domain, of human CD46 are crucial for infection of subgroup B adenovirus serotype 35. *J Control Release* 2006; 113: 271–278.
16 Wild TF, Buckland R. Functional aspects of envelope-associated measles virus proteins. *Curr Top Microbiol Immunol* 1995; 191: 51–64.
17 Schneider-Schaulies J, Schnorr JJ, Brinckmann U, Dunster LM, Baczko K, Liebert UG *et al*. Receptor usage and differential downregulation of CD46 by measles virus wild-type and vaccine strains. *Proc Natl Acad Sci USA* 1995; 92: 3943–3947.
18 Vogels R, Zuijdgeest D, van Rijnsoever R, Hartkoorn E, Damen I, de Bethune MP *et al*. Replication-deficient human adenovirus type 35 vectors for gene transfer and vaccination: efficient human cell infection and bypass of preexisting adenovirus immunity. *J Virol* 2003; 77: 8263–8271.
19 Roelvink PW, Lizonova A, Lee JG, Li Y, Bergelson JM, Finberg RW *et al*. The coxsackievirus-adenovirus receptor protein can function as a cellular attachment protein for adenovirus serotypes from subgroups A, C, D, E, and F. *J Virol* 1998; 72: 7909–7915.
20 Sakurai F, Mizuguchi H, Hayakawa T. Efficient gene transfer into human CD34+ cells by an adenovirus type 35 vector. *Gene Therapy* 2003; 10: 1041–1048.
21 Seshidhar Reddy P, Ganesh S, Limbach MP, Brann T, Pinkstaff A, Kaloss M *et al*. Development of adenovirus serotype 35 as a gene transfer vector. *Virology* 2003; 311: 384–393.
22 Abrahamsen K, Kong HL, Mastrangeli A, Brough D, Lizonova A, Crystal RG *et al*. Construction of an adenovirus type 7a E1A-vector. *J Virol* 1997; 71: 8946–8951.
23 Holterman L, Vogels R, van der Vlugt R, Sieuwerts M, Grimbergen J, Kaspers J *et al*. Novel replication-incompetent vector derived from adenovirus type 11 (Ad11) for vaccination and gene therapy: low seroprevalence and non-cross-reactivity with Ad5. *J Virol* 2004; 78: 13207–13215.
24 Sirena D, Ruzsics Z, Schaffner W, Greber UF, Hemmi S. The nucleotide sequence and a first generation gene transfer vector of species B human adenovirus serotype 3. *Virology* 2005; 343: 283–298.
25 Mizuguchi H, Hayakawa T. Adenovirus vectors containing chimeric type 5 and type 35 fiber proteins exhibit altered and expanded tropism and increase the size limit of foreign genes. *Gene* 2002; 285: 69–77.
26 Shayakhmetov DM, Papayannopoulou T, Stamatoyannopoulos G, Lieber A. Efficient gene transfer into human CD34(+) cells by a retargeted adenovirus vector. *J Virol* 2000; 74: 2567–2583.
27 Krasnykh VN, Mikheeva GV, Douglas JT, Curiel DT. Generation of recombinant adenovirus vectors with modified fibers for altering viral tropism. *J Virol* 1996; 70: 6839–6846.
28 Stecher H, Shayakhmetov DM, Stamatoyannopoulos G, Lieber A. A capsid-modified adenovirus vector devoid of all viral genes: assessment of transduction and toxicity in human hematopoietic cells. *Mol Ther* 2001; 4: 36–44.
29 Karp CL, Wysocka M, Wahl LM, Ahearn JM, Cuomo PJ, Sherry B *et al*. Mechanism of suppression of cell-mediated immunity by measles virus. *Science* 1996; 273: 228–231.
30 Smith A, Santoro F, Di Lullo G, Dagna L, Verani A, Lusso P. Selective suppression of IL-12 production by human herpesvirus 6. *Blood* 2003; 102: 2877–2884.
31 Schneider-Schaulies J, Schnorr JJ, Schlender J, Dunster LM, Schneider-Schaulies S, ter Meulen V. Receptor (CD46) modulation and complement-mediated lysis of uninfected cells after contact with measles virus-infected cells. *J Virol* 1996; 70: 255–263.
32 Lecouturier V, Rizzitelli A, Fayolle J, Daviet L, Wild FT, Buckland R. Interaction of measles virus (Halle strain) with CD46: evidence that a common binding site on CD46 facilitates both CD46 downregulation and MV infection. *Biochem Biophys Res Commun* 1999; 264: 268–275.
33 Iwata K, Seya T, Yanagi Y, Pesando JM, Johnson PM, Okabe M *et al*. Diversity of sites for measles virus binding and for inactivation of complement C3b and C4b on membrane cofactor protein CD46. *J Biol Chem* 1995; 270: 15148–15152.
34 Manchester M, Valsamakis A, Kaufman R, Liszewski MK, Alvarez J, Atkinson JP *et al*. Measles virus and C3 binding sites are distinct on membrane cofactor protein (CD46). *Proc Natl Acad Sci USA* 1995; 92: 2303–2307.

35 Bartz R, Firsching R, Rima B, ter Meulen V, Schneider-Schaulies J. Differential receptor usage by measles virus strains. *J Gen Virol* 1998; 79 (Part 5): 1015–1025.
36 Liszewski MK, Tedja I, Atkinson JP. Membrane cofactor protein (CD46) of complement. Processing differences related to alternatively spliced cytoplasmic domains. *J Biol Chem* 1994; 269: 10776–10779.
37 Oliaro J, Pasam A, Waterhouse NJ, Browne KA, Ludford-Menting MJ, Trapani JA *et al*. Ligation of the cell surface receptor, CD46, alters T cell polarity and response to antigen presentation. *Proc Natl Acad Sci USA* 2006; 103: 18685–18690.
38 Kemper C, Verbsky JW, Price JD, Atkinson JP. T-cell stimulation and regulation: with complements from CD46. *Immunol Res* 2005; 32: 31–43.
39 Harris CL, Spiller OB, Morgan BP. Human and rodent decay-accelerating factors (CD55) are not species restricted in their complement-inhibiting activities. *Immunology* 2000; 100: 462–470.
40 Sakurai F, Kawabata K, Koizumi N, Yamaguchi T, Hayakawa T, Mizuguchi H. Adenovirus serotype 35 vector-mediated transduction into human CD46-transgenic mice. *Gene Therapy* 2006; 13: 1118–1126.
41 Mizuguchi H, Koizumi N, Hosono T, Utoguchi N, Watanabe Y, Kay MA *et al*. A simplified system for constructing recombinant adenoviral vectors containing heterologous peptides in the HI loop of their fiber knob. *Gene Therapy* 2001; 8: 730–735.
42 Maizel Jr JV, White DO, Scharff MD. The polypeptides of adenovirus. I. Evidence for multiple protein components in the virion and a comparison of types 2, 7A, and 12. *Virology* 1968; 36: 115–125.
43 Koizumi N, Mizuguchi H, Hosono T, Ishii-Watabe A, Uchida E, Utoguchi N *et al*. Efficient gene transfer by fiber-mutant adenoviral vectors containing RGD peptide. *Biochim Biophys Acta* 2001; 1568: 13–20.
44 Sakurai F, Kawabata K, Yamaguchi T, Hayakawa T, Mizuguchi H. Optimization of adenovirus serotype 35 vectors for efficient transduction in human hematopoietic progenitors: comparison of promoter activities. *Gene Therapy* 2005; 12: 1424–1433.
45 Rushmere NK, Knowlden JM, Gee JM, Harper ME, Robertson JF, Morgan BP *et al*. Analysis of the level of mRNA expression of the membrane regulators of complement, CD59, CD55 and CD46, in breast cancer. *Int J Cancer* 2004; 108: 930–936.
46 Dash S, Saxena R, Myung J, Rege T, Tsuji H, Gaglio P *et al*. HCV RNA levels in hepatocellular carcinomas and adjacent non-tumorous livers. *J Virol Methods* 2000; 90: 15–23.

—Review—

35型アデノウイルスベクターの開発—遺伝子改変動物並びに霊長類を用いた検討—

櫻井文教,*,[a] 川端健二,[a] 水口裕之[a,b]

Characterization of Adenovirus Serotype 35 Vectors Using Genetically Modified Animals and Nonhuman Primates

Fuminori SAKURAI,*,[a] Kenji KAWABATA,[a] and Hiroyuki MIZUGUCHI[a,b]

[a]*Laboratory of Gene Transfer and Regulation, National Institute of Biomedical Innovation, 7-6-8 Asagi, Saito, Ibaragi City 567-0085, Japan, and* [b]*Graduate School of Pharmaceutical Sciences, Osaka Univerisity, 1-6 Yamadaoka, Suita City 565-0871, Japan*

(Received June 29, 2006)

Recombinant Adenovirus (Ad) vectors are considered to be a promising gene delivery vehicle of high utility because they are easy to construct, can be produced at high titers, and efficiently transduce various types of cells. Ad vectors commonly used in the world, including clinical trials, are composed of Ad serotype 5 (Ad5), which belongs to subgroup C. In recent years, however, it has become apparent that Ad5 vectors have some drawbacks, such as high seroprevalence of anti-Ad5 antibodies in adults and low transduction efficiencies of Ad5 vectors in cells lacking a primary receptor for Ad5, coxsackievirus and adenovirus receptor (CAR). To overcome these limitations of Ad5 vectors, we have developed a novel type of Ad vector, which is composed of Ad serotype 35 (Ad35), belonging to subgroup B. Ad35 vectors recognize human CD46, not CAR, as a cellular receptor for infection. Human CD46 is expressed in almost all of human cells, leading to a broad tropism of Ad35 vectors to human cells, in contrast, expression of rodent CD46 is limited to the testis. Therefore, *in vivo* transduction properties of Ad35 vectors are not appropriately evaluated in normal mice. In order to evaluate the *in vivo* transduction properties of Ad35 vectors, Ad35 vectors were applied to human CD46-transgenic mice and nonhuman primates, which express CD46 in a similar pattern to humans. The data obtained using CD46-transgenic mice and nonhuman primates would provide valuable information towards clinical applications of Ad35 vectors.

Key words——adenovirus vectors; serotype; CD46; gene therapy

1. はじめに

遺伝子治療では遺伝子（核酸）が薬物（主剤）そのものであると考えられるが，通常の薬物とは異なり，多くの場合分子量 10^6 以上の巨大高分子である遺伝子を疾患部位の細胞の核にまで到達させる必要がある．したがって，遺伝子を細胞内，そして核内にまで送達するベクターが遺伝子治療の成否を決める極めて重要な要素であると言っても過言ではない．遺伝子導入用ベクターは，ウイルスを基本骨格としウイルス本来が兼ね備えている遺伝子送達メカニズムを利用したウイルスベクターと，脂質や高分子ポリマーを利用した非ウイルスベクターとに大別される．これまでウイルス・非ウイルスベクターを問わず多くの遺伝子導入用ベクターが開発されてきたが，なかでもアデノウイルス（Ad）ベクターは遺伝子導入用ベクターとして多くの長所を有することから，様々なアプローチからベクター改良研究が盛んに行われている．

Adは軽い風邪を引き起こすウイルスの1つで，約 36 kb の直鎖状二本鎖 DNA をゲノムに持つエンベロープを持たないウイルスである．その形状は Fig. 1 に示すように，直径約 80 nm の正二十面体構造をしており，その頂点には感染に大きな役割を担っている 12 個のペントン（ファイバー及びペントンベース）と呼ばれる突起構造を持っている．Adはこれまで多くの動物から単離されているが，ヒト Ad は現在までに 51 種類の血清型が同定されており，赤血球凝集活性の違いなどから A—F の 6 つの Subgroup に分類されている（Table 1）.[1] 現在汎用

[a]独立行政法人医薬基盤研究所遺伝子導入制御プロジェクト（〒567-0085 茨木市彩都あさぎ 7-6-8），[b]大阪大学大学院薬学研究科（〒565-0871 吹田市山田丘 1-6）
*e-mail: sakurai@nibio.go.jp

本総説は，日本薬学会第 126 年会シンポジウム S7 で発表したものを中心に記述したものである．

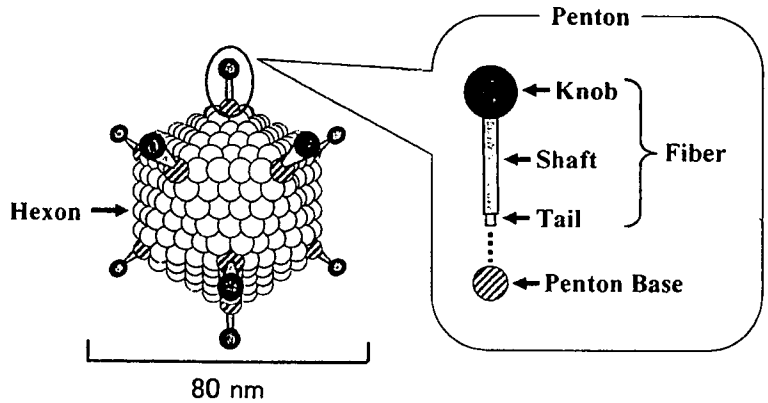

Fig. 1. A Schematic Diagram of Human Adenovirus
The double-stranded genomic DNA is packaged in the icosahedral particle with fibers projecting from the twelve vertices.

Table 1. Human Adenovirus Serotypes

Subgroup	Serotypes	Receptor*)
A	12, 18, 31	CAR
B	3, 7, 11, 14, 16, 21, 34, 35, 50	CD46
C	1, 2, 5, 6	CAR
D	8-10, 13, 15, 17, 19, 20, 22-30, 32, 33, 36-39, 42-49, 51	CAR
E	4	CAR
F	40, 41	CAR

CAR: coxsackievirus-adenovirus receptor. *) Some Ad serotypes recognize other receptors different from CAR and CD46.

されているAdベクターはSubgroup Cに属する5型Ad（若しくは2型）を基本骨格としている．5型Adベクターは全遺伝子治療臨床研究の約25%で用いられており（2006年1月現在），最近では遺伝子機能解析のためのツールとして基礎研究の場においても汎用されている．しかし近年，後述するように5型Adベクターの抱える様々な問題が明らかとなってきた．そこでわれわれは5型Adベクターの問題点を解決すべく，Subgroup Bに属する35型Adを基本骨格とした新規Adベクターを開発し，その機能解析を進めている．[2—6] 本稿では，われわれがこれまでに取り組んできた研究成果について紹介したいと思う．

2. 5型アデノウイルスベクターの問題点

1993年にアメリカにおいて嚢胞性繊維症に対して行われた5型Adベクターによる初めての臨床試験以降，[7] 5型Adベクターは癌や先天性遺伝子疾患などの臨床研究や多くの基礎研究に用いられてきた．これらの研究は5型Adベクターの有用性を示すと同時に，以下に示すような5型Adベクターが抱える問題点を明らかにした．

1）第一受容体であるCoxsackievirus and adenovirus receptor（CAR）の発現が低い細胞への遺伝子導入効率が低い．CARは1997年にBergelsonらによって2型及び5型Ad及びCoxsackie B virusの受容体として同定された分子量約46 KDaの膜タンパク質で，[8] 上皮細胞や肝細胞などで多く発現している．Subgroup Bに属するAdを除くほぼすべてのAdがCARを第一受容体としている．[9] したがって5型AdベクターはCAR陽性細胞に対しては効率よく感染し高い遺伝子導入効率を示すが，CAR陰性細胞では十分な遺伝子導入効率が得られない．CAR陰性細胞は意外にも多く，遺伝子治療の重要な標的細胞である造血幹細胞を始めとする血液細胞，血管平滑筋細胞，樹状細胞などがCAR陰性である．また癌細胞においては，癌の悪性度の進行に伴いCARの発現が低下することが報告されている．[10,11] さらに最近の研究ではCARがタイトジャンクションの形成に関与することが報告されており，[12,13] CAR陽性細胞においてもCARがタイトジャンクション部位に局在している場合には，立体障

櫻井文教

独立行政法人医薬基盤研究所遺伝子導入制御プロジェクト研究員．1972年静岡県生まれ．京都大学薬学部卒業．京都大学大学院薬学研究科博士課程修了（指導教官　橋田充教授）．2001年国立医薬品食品衛生研究所生物薬品部リサーチレジデント（早川堯夫部長）．2003年国立医薬品食品衛生研究所遺伝子細胞医薬部研究員（山口照英部長）．2005年より現職（水口裕之プロジェクトリーダー）．

害により5型Adベクターが CARに到達できない可能性が指摘されている.

2) 既に多くの成人が5型Adに対する抗体を保持している. 5型Adは風邪の原因ウイルスの1つであることが知られており, 成人の多くは5型Adに対する抗体を既に有している. Seshidharらは, 成人の45—66%は5型Adに対する抗体を保持していると報告している.[14] 既存抗体は *in vivo* 遺伝子導入効率を大きく減弱させるだけでなく, 5型Adベクターの毒性を増強する可能性が指摘されている.[15] すなわち, 抗5型Ad抗体を保持しているヒトに5型Adベクターを投与した場合には, 抗体により遺伝子導入が阻害され十分な治療効果が得られないだけでなく, 大きな副作用を起こす危険性がある.

3. 35型アデノウイルスベクターの特徴

以上のような問題点を克服するため, われわれはSubgroup Bに属する35型Adを基本骨格とした新規Adベクターの開発を行った. 35型Adのベクター化に着目した理由としては (Fig. 2),

1) 受容体としてヒトCD46 (membrane cofactor protein) を認識して細胞に感染するため, 5型Adとは異なる感染域を示す. 35型Adを始めとするSubgroup Bに属するAdの受容体は長らく不明であった (われわれが35型Adベクターの開発に成功した時点においても不明であった). しかしながら35型Adがcar以外の分子を受容体として認識すること,[9] 血球細胞に対し高い親和性を有すること[16]が既に明らかとなっていたことから, われわれは35型Adベクターが血液細胞を始めとして5型Adベクターでは遺伝子導入不可能な細胞に対しても効率よく感染するのではないかと考えた. 実際に開発した35型Adベクターの遺伝子導入特性を解析したところ, 35型AdベクターはCAR陽性細胞だけでなく, ヒトCD34陽性細胞を始めとするCAR陰性細胞に対しても高い遺伝子導入効率を示した.[2—4] その後2003年にヒトCD46がSubgroup B Adの受容体であることが報告されたが,[17,18] CD46はヒトではほぼすべての細胞で発現しており, 35型Adベクターの広い感染域を反映したものであった.

2) 35型Adに対する抗体を保持している成人の割合が低い. 先述のように成人の抗5型Ad抗体保持率は45%以上であるが, Subgroup B Adに対する抗体保持率は総じて低いことが報告されている. 特に35型Adに対する抗体保持率は20%以下と低いことから,[14,19] 35型Adベクターの遺伝子導入活性が既存抗体により阻害される可能性は低い. また35型Adは5型Adとは異なるSubgroupに属することから, 抗5型Ad抗体による阻害を受けない. われわれが抗5型Ad血清存在下における5型並びに35型Adベクターの遺伝子導入効率を検討した

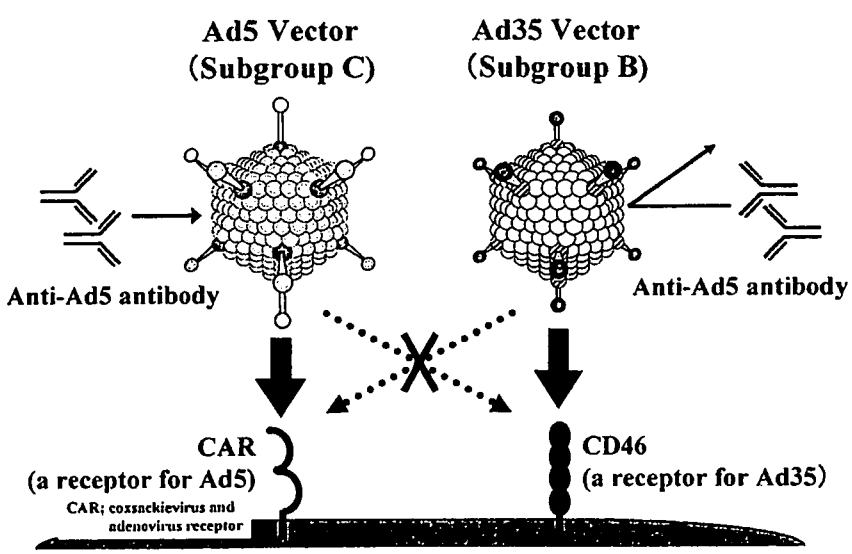

Fig. 2. A Schematic Diagram of Properties of Ad5 and Ad35 Vectors

Ad5 vectors infect cells via interaction with CAR (coxsackievirus and adenovirus receptor), on the other hand, Ad35 vectors recognize human CD46 for infection. Anti-Ad5 antibodies inhibit infection of Ad5 vectors, not Ad35 vectors.

ところ，5型Adベクターの遺伝子導入効率は抗5型Ad血清の濃度依存的に減少したが，35型Adベクターの遺伝子導入効率は影響を受けなかった．

一方で，ファイバータンパク質だけを35型Adなどの Subgroup Bに属するAdに由来するものに置換し，その他の領域は従来の5型Adから構成されたファイバー置換型5型Adベクターも開発されている．[20,21] ファイバーの先端部分であるノブ領域がCD46に直接結合する部位であることから，ファイバータンパク質のみを置換することで感染域を変えることが可能である．しかしほとんどの抗Ad中和抗体はヘキソン領域を認識するため，[22] ファイバー置換型5型Adベクターでは抗5型Ad抗体による阻害を回避することはできない．

4. CD46の特徴

Subgroup B Adの受容体であるCD46は，主に4つのisoform（BC1, BC2, C1, C2）が存在する分子量約55—65 KDaの糖タンパク質で，4つのShort consensus repeat（SCR），transmembrane domain, cytoplasmic tailなどから構成されている(Fig. 3)．CD46は本来，生体では補体成分であるC3bやC4bを分解することにより，自己の細胞を補体による攻撃から守る役割を担っている．またSubgroup B Adのみならず，麻疹ウイルス（一部のstrain），ヒトヘルペスウイルスtype 6, Nesseriaなども CD46を感染受容体としている．[23,24] これらの病原体についてはCD46のどの部位が感染に関与するのかが報告されており，Subgroup B Adについても先端領域に位置するSCR1及び2が感染に重要であることが明らかとなっている．[6,25] CARとは異なり，CD46はヒトでは血液細胞を始め，ほぼすべての細胞において発現しているのに対し（赤血球では発現していない），げっ歯類においてはCD46は精巣でしか発現していないこと，またマウスCD46はヒトCD46と比較してその相同性は約46%と低いことが知られている．[26] そのため35型Adベクターを通常のマウスに静脈内投与した場合の各臓器における遺伝子導入効率は，5型Adベクターと比較し極めて低いものであった．[3]

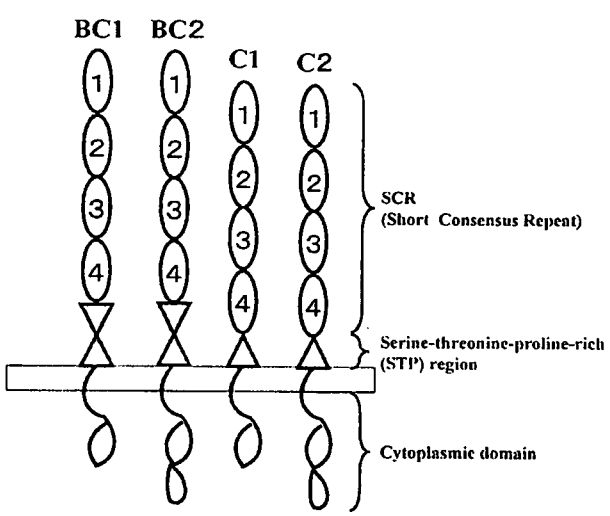

Fig. 3. A Schematic Diagram of Human CD46

Human CD46 is ubiquitously expressed in almost all human cells mainly as four isoforms (BC1, BC2, C1, C2) that are derived via alternative splicing. Human CD46 is composed of four cysteine-rich short consensus repeats (SCRs), a serine-threonine-proline-rich (STP) region, a short region of unknown function, a hydrophobic transmembrane domain, and a carboxy-terminal cytoplasmic domain.

5. CD46トランスジェニックマウスを用いた35型Adベクターの機能解析

そこでわれわれは，35型Adベクターが通常のマウスで遺伝子発現を示さないのは，受容体であるCD46が発現していないことが原因ではないかと考え，ヒトと同様にヒトCD46をほぼ全臓器で発現しているCD46トランスジェニック（CD46TG）マウス（大阪大学・岡部勝先生より供与）を用いて35型Adベクターの遺伝子導入特性を解析した．[5] まずCD46TGマウスにおけるCD46発現量をウエスタンブロットにて確認したところ，ヒトと同様にほぼすべての臓器でCD46の発現が確認された．次に35型Adベクターを野生型及びCD46TGマウスに静脈内及び腹腔内投与したところ，両投与経路ともにCD46TGマウスにおいて野生型マウスよりも有意に高い遺伝子導入効率が得られた（Fig. 4）．特に，両方の相同染色体にCD46遺伝子を有するホモCD46TGマウスの肝臓での遺伝子導入効率は，静脈内投与では野生型マウスの約10倍，腹腔内投与では約500倍高い値を示した．しかしながら，5型Adベクターと比較して，35型Adベクターによる遺伝子導入効率はCD46TGマウスにおいても依然低く，実験当初に期待していたような劇的な遺伝子導入効率の上昇はみられなかった．例えば35型Adベクターをホモ CD46TGマウスに静脈内投与したときの肝臓及び脾臓での遺伝子発現量は，5型Adベクターを野生型マウスに静脈内投与した場合のそれぞれ約20000分の1，及び50分の1であった．さらに35型Adベクターを CD46TGマウスに

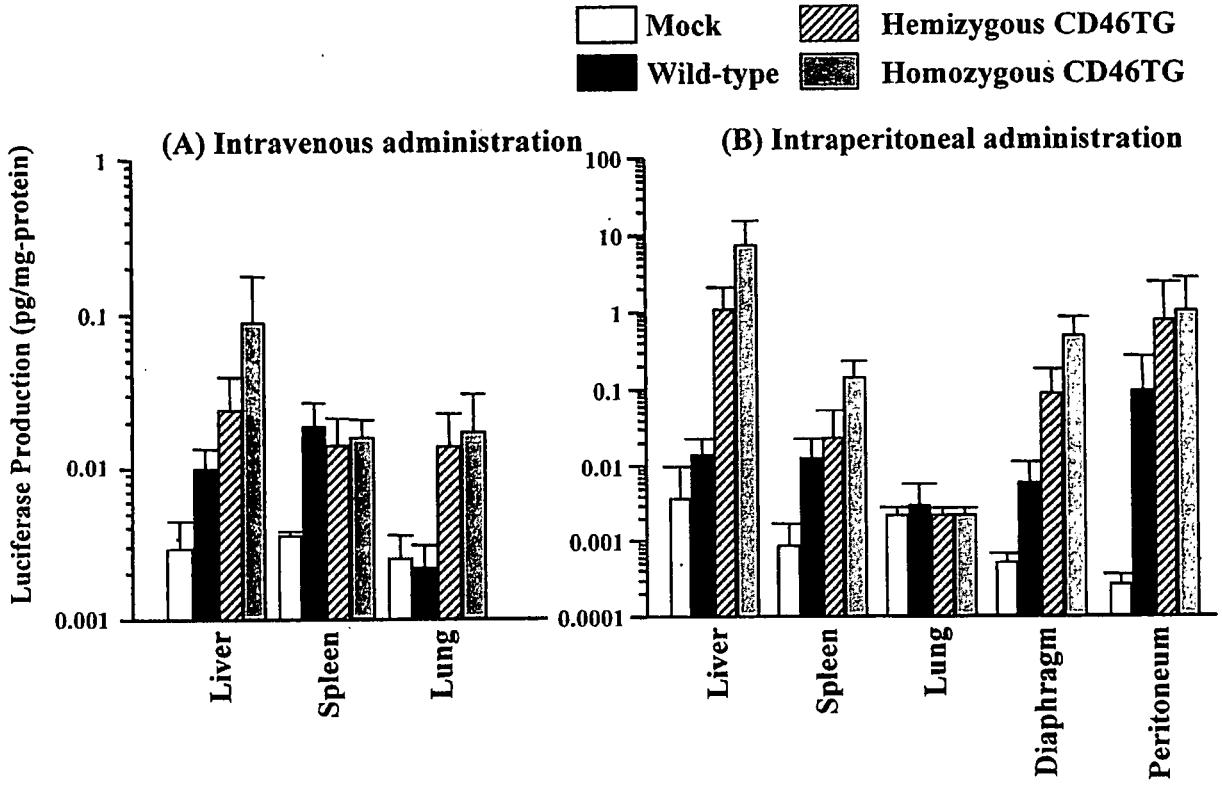

Fig. 4. Luciferase Production in CD46TG and Wild-type Mice after Intravenous and Intraperitoneal Administration of Ad35 Vectors Expressing Firefly Luciferase

(A) Luciferase production in the organs after intravenous administration of Ad35 vectors. (B) Luciferase production in the organs after intraperitoneal administration of Ad35 vectors. Ad35 vectors (1.5×10^{10} VP) was administered to wild-type mice (C57Bl6, 5 weeks old) and hemizygous (Hemi TG, 5 to 6 weeks old) and homozygous (Homo TG, 5 to 6 weeks old) CD46TG mice. After 48 h, the organs were harvested and homogenized, and luciferase production was measured by a luminescence assay system (PicaGene 5500; Toyo Inki, Japan). All data are represented as mean±S.D. ($n=4$, intravenous administration; $n=6$, intraperitoneal administration).

腹腔内投与した場合に遺伝子発現を示した細胞の大部分は臓器表面の中皮細胞であった（Fig. 5）.

6. カニクイザルを用いた35型Adベクターの機能解析

35型Adベクターは CD46TG マウスにおいても十分な遺伝子発現を示さなかったが，これに関しては主に2つの原因が推察された．第一に CD46 が主に basolateral 側に発現しているために，[27] 細胞外マトリックスなどの立体障害により35型Adベクターが CD46 に到達できないことが考えられた．あるいは，35型Ad には CD46 以外の未知の受容体の存在が示唆されているが，[28] マウスではその受容体が発現していない可能性があった．そこでわれわれは，ヒトと同様に生来から CD46 を発現している霊長類を用いて35型Adベクターの機能評価を行った．35型Adベクターをカニクイザルに静脈内投与し，投与96時間後の各臓器における遺伝子発現並びにベクター集積量を検討した．その結果，35型Adベクターのゲノム DNA は肝臓で最も多く検出され，その他，肺，腎臓，心臓においても高い値を示した．一方で各臓器における遺伝子発現を検討したところ，ほとんど遺伝子発現は観察されず，CD46TG マウスを用いた場合と同様の傾向を示した．今後われわれは霊長類を用いて35型Adベクターの機能解析をさらに進めるとともに，臓器局所への投与による遺伝子導入実験も計画している．これらの実験により35型Adベクターの臨床応用に向けて重要な知見が得られるものと期待している．

7. おわりに

以上，本稿ではわれわれが開発した新しいタイプの Ad ベクターである35型Adベクターの機能解析（遺伝子導入特性解析）を遺伝子改変動物並びに霊長類を用いて行った研究について紹介した．遺伝子治療研究が始まって以来，精力的に基礎研究並びに臨床試験が進められ，貴重な数多くの情報が蓄積されてきた．今，これらの情報は高性能なベクター